Regular Article – Theoretical Physics

The electromagnetic Sigma-to-Lambda hyperon transition form factors at low energies

Carlos Granados[1,2], Stefan Leupold[1,a], and Elisabetta Perotti[1]

[1] Institutionen för fysik och astronomi, Uppsala Universitet, Box 516, S-75120 Uppsala, Sweden
[2] Jefferson Lab, 12000 Jefferson Ave., Newport News, VA 23606, USA

Abstract. Using dispersion theory the low-energy electromagnetic form factors for the transition of a Sigma to a Lambda hyperon are related to the pion vector form factor. The additionally required input, *i.e.* the two-pion–Sigma–Lambda amplitudes are determined from relativistic next-to-leading-order (NLO) baryon chiral perturbation theory including the baryons from the octet and optionally from the decuplet. Pion rescattering is again taken into account by dispersion theory. It turns out that the inclusion of decuplet baryons is not an option but a necessity to obtain reasonable results. The electric transition form factor remains very small in the whole low-energy region. The magnetic transition form factor depends strongly on one not very well determined low-energy constant of the NLO Lagrangian. One obtains reasonable predictive power if this low-energy constant is determined from a measurement of the magnetic transition radius. Such a measurement can be performed at the future Facility for Antiproton and Ion Research (FAIR).

1 Introduction

The quest to understand the structure of matter does not stop with identifying the building blocks of a composite object. One wants to understand quantitatively how the respective building blocks interact and how they are distributed inside of this composite object. Some possible ways to explore the intrinsic structure of an object are

a) to excite it,
b) to scatter on it,
c) to replace some of its building blocks by other, similar ones.

In atomic physics all these techniques produced key insights and cross-checks of our understanding, for instance by studying the hydrogen spectrum —related to a), by Rutherford scattering —related to b), or by studying systems with different atomic nuclei but the same number of electrons or electronic *versus* muonic atoms —related to c).

To explore the structure of the nucleon one proceeds along similar lines. Concerning the excitation spectrum an increasing number of nucleon resonances has been isolated over the past decades [1]. The motivation of the present

work, however, derives more from an interplay of the approaches b) and c). A huge body of information has been obtained from electron-nucleon scattering [2] and related observables —with the most recent clue of an apparent difference in the proton charge radius as extracted from electronic or muonic hydrogen, respectively [3,4]. The central objects are the electromagnetic form factors and the corresponding low-energy quantities: electric charge, magnetic moment, electric and magnetic radii. We note in passing that the non-trivial magnetic moment of the proton provided one of the first hints on the intrinsic structure of the proton [5]. If one flips the spin of one of the quarks inside the nucleon, one obtains a Delta baryon[1]. The quantities extracted from the scattering reactions electron-nucleon to electron-Delta are the Delta-to-nucleon transition form factors. Extrapolating to the photon point one obtains the helicity amplitudes [1]. The transition form factors provide complementary information about the structure of the nucleon (and the Delta) and have also been studied in some detail [6].

The lightest quarks, up and down, provide the constituent-quark content of nucleon and Delta. Yet there is one more comparatively light quark, the strange quark. In

---

a e-mail: stefan.leupold@physics.uu.se

[1] One might interpret this spin flip in the sense of an excitation a) or a replacement c), but in this case this classification is merely language, not content.

the spirit of approach c) one can ask what changes about the nucleon (and/or the Delta) if one or several up or down quarks are replaced by strange quarks. Historically, the such obtained states, the hyperons, were instrumental in revealing the quarks as the building blocks of the nucleons and other hadrons [7]. This suggests that the intrinsic structures of hyperons and nucleons are intimately related. Obviously, hyperon electromagnetic form factors and transition form factors contain complementary information to the nucleon and Delta form factors. Their knowledge would provide tests for our current picture of the nucleon structure and therefore deepen our understanding. At low energies one can address the question how well three-flavor chiral perturbation theory converges [8]. At intermediate energies phenomenological models of the nucleon might be capable to predict how the nucleon structure changes when a light quark is replaced by a strange quark. Such predictions can be scrutinized by hyperon data. At large momenta one is interested to see where quark-number scaling [9] sets in and to which extent this onset depends on the strange-quark mass. In general, systems with strangeness address the interplay of dynamically generated and explicit mass since the strange-quark mass is comparable to the dynamical scale set by Λ_{QCD} [1]. Yet, the experimental information about hyperon form factors is rather limited. Concerning low-energy data, essentially only the magnetic moments of the octet hyperons are known (and, of course, their charges) [1]. For the decuplet-octet transitions not even the helicity amplitudes have been determined.

Of course, this present limitation in the knowledge about hyperon form factors is caused by the fact that octet hyperons are not stable, but decay on account of the weak interaction [1]. Therefore hyperon-electron scattering is experimentally very difficult to realize. Yet, the crossing symmetry of relativistic quantum fields provides a new angle. While electron-baryon scattering probes the form factors in the space-like region, hyperon form factors are accessible in the time-like[2] region for high and low energies. For high energies one can study electron-positron scattering reactions to a hyperon and an anti-hyperon. In principle, "direct" form factors and transition form factors are accessible here. For low energies one can extract transition form factors from the Dalitz decays $Y \rightarrow Y' e^+ e^-$ where Y and Y' denote two distinct hyperons. Of course, it is a shortcoming that the space-like region of the form factors is not easily accessible for hyperons. However, to some extent there is a compensation for it. The weak decays of the hyperons are self-analyzing in the sense that the angular distributions of the decay products give access to the spin properties without explicit polarization. Thus one might get an easier access to the various form factors as compared to the nucleon and Delta-nucleon cases.

In the present and forthcoming works we will address electromagnetic form factors of hyperons at low energies

from the theory side. The calculations will cover the whole space- and time-like low-energy region, but at present the experimental significance resides in the time-like Dalitz-decay region. Such electromagnetic decays of hyperons could be studied with high statistics at the future Facility for Antiproton and Ion Research (FAIR) at Darmstadt, Germany. There, hyperons will be copiously produced in $\bar{p}\,p$ (PANDA [10]) and $p\,p$ (HADES[3]) collisions. In the present work we study the only form factors in the octet sector that are connected to a Dalitz decay, namely the electric and the magnetic transition form factor of the neutral Σ^0 hyperon to the Λ hyperon. These transition form factors are accessible by high-precision measurements of the decay $\Sigma^0 \rightarrow \Lambda\, e^+ e^-$.

The main part of the present work deals with the calculation of these transition form factors. However, some discussion about the experimental feasibility is appropriate: The transition form factors are functions of the invariant mass of the dilepton, *i.e.* of the $e^+ e^-$ system. To resolve the shape of a form factor requires some range of invariant masses. For the Dalitz decay $\Sigma^0 \rightarrow \Lambda\, e^+ e^-$ the upper limit of available invariant masses is given by $m_{\Sigma^0} - m_\Lambda \approx 77\,\mathrm{MeV}$. This is not very large as compared to typical hadronic scales. Thus, to extract even the electric or magnetic transition radius —the first non-trivial aspect of a form factor— requires a high experimental precision. In addition, the extraction of these radii from decay data relies on a proper understanding of the electromagnetic part. The lowest-order QED part is easily worked out. However, if the impact of the hyperon transition form factors/radii is numerically small, then radiative QED corrections compete with the hadronic form-factor effects. This interplay will be explored in [12]. In the present work we concentrate on the hadronic part, the calculation of the hyperon electromagnetic form factors for the transition Σ^0 to Λ.

Chiral perturbation theory (χPT) provides a model-independent approach to low-energy QCD [13–17]. Beyond the pseudo-Goldstone bosons it is possible to include the baryon octet and maybe the decuplet [6,18,19], but it is unclear how to treat other hadronic states in a systematic, model-independent way. In the interaction of hadrons with electromagnetism the vector mesons turn out to be very prominent [20]. For the isovector case the ρ meson influences the electromagnetic structure down to rather low energies. Experimentally the ρ meson shows up as a resonance in the p-wave pion phase shift and in the pion form factor. Both quantities are nowadays known to high precision [21–24]. Therefore one might pursue the strategy to marry purely hadronic χPT with the experimentally known pion form factor. Dispersion theory allows to combine these ingredients. This is similar in spirit to [24–28]. Concerning nucleon form factors see also [29–31]. In purely hadronic χPT we will explore the options to consider explicitly the decuplet states as active degrees of freedom or to include them only indirectly via the low-energy constants of the next-to-leading order Lagrangian.

---

[2] Since there is some confusion in the literature we define these phrases explicitly; time-like/space-like means: modulus of energy larger/smaller than modulus of three-momentum.

[3] P. Salabura, private communication; see also [11] and references therein.

In the present work these ideas are applied to the Σ^0-to-Λ transition form factors. In contrast to elastic form factors the transition has the advantage that it is purely isovector. Therefore it provides a good first test case for our formalism. A direct calculation in relativistic three-flavor χPT has been performed in [8]. Therefore we can check the accuracy of the obtained results before extending it to other more involved cases. As next steps one could address in the future the transition of the decuplet Σ ($J^P = \frac{3}{2}^+$) to the Λ hyperon and of the Δ to the nucleon (for the latter case, see also [6]). Inclusion of the isosinglet part of electromagnetism opens the way for all elastic and transition form factors of octet and decuplet hyperons. Of course, at least for the calculations with the decuplet hyperons as initial states —as appropriate for the corresponding Dalitz decays— one has to use a version of χPT that includes the decuplet states as active degrees of freedom. But, as we will see, the results obtained in the present work suggest this anyway.

The rest of the paper is structured as follows: In the next section the theoretical ingredients are described in detail. Section 3 provides the results. Thereafter a summary and an outlook are presented. Appendices are added to discuss technical aspects and cross-checks which would interrupt the main text too much.

2 Ingredients

2.1 Dispersive representations

To apply dispersion theory we formally study the reaction $\Sigma^0 \bar\Lambda \to \gamma^*$, saturate the intermediate states by a pion pair and in the end extend the amplitude to the kinematical region $\Sigma^0 \to \Lambda \gamma^*$. Technically this is along the lines described, *e.g.*, in [28] based on [32,33]. We expect that the saturation of the inelasticity by a pion pair provides a good approximation for the transition form factors at low energies.

The form factors are defined in [8]. For our case of interest this reads

$$\langle 0|j^\mu|\Sigma^0 \bar\Lambda\rangle = e\,\bar v_\Lambda \left(\left(\gamma^\mu + \frac{m_\Lambda - m_\Sigma}{q^2}\, q^\mu\right) F_1(q^2) \right.$$
$$\left. - \frac{i\sigma^{\mu\nu}\, q_\nu}{m_\Lambda + m_\Sigma}\, F_2(q^2) \right) u_\Sigma \qquad (1)$$

with

$$G_E(q^2) := F_1(q^2) + \frac{q^2}{(m_\Sigma + m_\Lambda)^2}\, F_2(q^2),$$
$$G_M(q^2) := F_1(q^2) + F_2(q^2). \qquad (2)$$

q^2 denotes the square of the invariant mass of the virtual photon. With the conventions of (1) the photon momentum q is given by the sum of the momenta of the two hyperons. $G_{E/M}$ is called electric/magnetic transition form factor, $F_{1/2}$ is called Dirac/Pauli transition form factor. The transition form factors are chosen such that they fit

to the direct form factors that are commonly introduced for the baryon octet [8]. The appearance of $1/q^2$ in (1) in connection with F_1 enforces the vanishing of F_1 and therefore of G_E at the photon point, *i.e.* $G_E(0) = 0$.

To determine $G_M(0) = F_2(0)$ we use the experimental result for the decay $\Sigma^0 \to \Lambda\gamma$. It is governed by the matrix element

$$\mathcal{M} = \bar u_\Lambda\, \frac{e i\sigma_{\mu\nu} q^\nu}{m_\Lambda + m_\Sigma}\, \kappa\, u_\Sigma\, \varepsilon^\mu \qquad (3)$$

with $\kappa = G_M(0)$ [8]. The decay width is given by

$$\Gamma_{\Sigma^0 \to \Lambda\gamma} = \frac{e^2\, \kappa^2\, (m_\Sigma^2 - m_\Lambda^2)^3}{8\pi\, m_\Sigma^3\, (m_\Lambda + m_\Sigma)^2}, \qquad (4)$$

which leads to $\kappa \approx 1.98$ in agreement with the particle-data-group (PDG) value [1]

$$\mu := \kappa\, \frac{e}{m_\Lambda + m_\Sigma} = \kappa\, \underbrace{\frac{2m_P}{m_\Lambda + m_\Sigma}}_{\approx 1.61}\, \frac{e}{2m_P}. \qquad (5)$$

For later use we introduce the electric and magnetic transition radii [8]:

$$\langle r_E^2\rangle := 6\, \left.\frac{\mathrm{d}G_E(q^2)}{\mathrm{d}q^2}\right|_{q^2=0} \qquad (6)$$

and

$$\langle r_M^2\rangle := \frac{6}{G_M(0)}\, \left.\frac{\mathrm{d}G_M(q^2)}{\mathrm{d}q^2}\right|_{q^2=0}. \qquad (7)$$

For the dispersive representation of the form factors utilizing the two-pion intermediate state one needs a partial-wave decomposition [34] and an evaluation of the form factors and of the four-point amplitude $\Sigma^0 \bar\Lambda \pi^+ \pi^-$ for different helicity states. It is convenient to work in the center-of-mass frame, choose the z axis along the direction of motion of the Σ^0 and choose the z-x plane as the reaction plane. The corresponding spinors are explicitly given, *e.g.*, in [35]. So basically one needs to evaluate $\bar v_\Lambda(-p_z, \lambda)\, \Gamma\, u_\Sigma(p_z, \sigma)$ where Γ is an arbitrary spinor matrix and σ and λ denote the helicities. Because of parity invariance it is sufficient to evaluate this object for the two cases $\sigma = \lambda = +1/2$ and $\sigma = -\lambda = +1/2$. Concerning the form factors, for a given combination of helicities one obtains an amplitude $F(q^2, \sigma, \lambda)$ that is a superposition of the two form factors. In turn one can reconstruct the form factors from combinations of these amplitudes.

In the center-of-mass frame all components of the current in (1) vanish for $\sigma = \lambda = +1/2$ except for $\mu = 3$. One obtains

$$F(q^2, +1/2, +1/2) =$$
$$\bar v_\Lambda(-p_z, +1/2)\, \gamma^3\, u_\Sigma(p_z, +1/2)\, G_E(q^2). \qquad (8)$$

For $\sigma = -\lambda = +1/2$ all components vanish except for $\mu = 1, 2$ which are just related by a factor of i. One finds

$$F(q^2, +1/2, -1/2) =$$
$$\bar v_\Lambda(-p_z, -1/2)\, \gamma^1\, u_\Sigma(p_z, +1/2)\, G_M(q^2). \qquad (9)$$

It is convenient and avoids kinematical singularities if one divides out the respective spinor coefficient and formulates dispersion relations directly for the electric and magnetic form factor. However, one should first consider for which pair of the four quantities G_E, G_M, F_1 and F_2 one would like to set up a (low-energy) dispersive representation. Concerning a direct χPT calculation it has been proposed in [8] to use the Dirac and Pauli form factor F_1 and F_2. From the point of view of our helicity decomposition the electric and magnetic form factor seem to be more direct. In principle, if one has an excellent input for all these quantities, it should not matter. In reality, however, the relations (2) mix different powers of q^2 which is an issue in a necessarily truncated low-energy expansion in powers of momenta. In the present work we will use the electric and magnetic form factor as a starting point. We have briefly explored the option to start with dispersive representations for the Dirac and Pauli form factor, but with the next-to-leading-order input of chiral perturbation theory the results were less convincing. Clearly this deserves more detailed studies in the future.

We will mainly use the subtracted dispersion relations (see also [24])

$$
G_{M/E}(q^2) = G_{M/E}(0) \\
+ \frac{q^2}{12\pi} \int_{4m_\pi^2}^\infty \frac{\mathrm{d}s}{\pi} \frac{T_{M/E}(s)\, p_{\mathrm{c.m.}}^3(s)\, F_\pi^{V*}(s)}{s^{3/2}\,(s - q^2 - i\epsilon)}\,.
$$
(10)

The subtraction constants that appear in (10) can be adjusted to match the form factors at the photon point, $G_E(0) = 0$, $G_M(0) = \kappa$. In line with the names for the form factors we will denote the corresponding amplitudes T_E and T_M by electric and magnetic scattering amplitude, respectively.

We might also examine an unsubtracted version

$$
G_{M/E}(q^2) = \frac{1}{12\pi} \int_{4m_\pi^2}^\infty \frac{\mathrm{d}s}{\pi} \frac{T_{M/E}(s)\, p_{\mathrm{c.m.}}^3(s)\, F_\pi^{V*}(s)}{s^{1/2}\,(s - q^2 - i\epsilon)}
$$
(11)

and explore to which extent the pion loop plus pion rescattering saturates the magnetic moment of the transition,

$$
\kappa \stackrel{?}{=} \frac{1}{12\pi} \int_{4m_\pi^2}^\infty \frac{\mathrm{d}s}{\pi} \frac{T_M(s)\, p_{\mathrm{c.m.}}^3(s)\, F_\pi^{V*}(s)}{s^{3/2}}\,,
$$
(12)

or to which extent the dispersively calculated "charge" vanishes:

$$
0 \stackrel{?}{=} \frac{1}{12\pi} \int_{4m_\pi^2}^\infty \frac{\mathrm{d}s}{\pi} \frac{T_E(s)\, p_{\mathrm{c.m.}}^3(s)\, F_\pi^{V*}(s)}{s^{3/2}}\,.
$$
(13)

In general we expect that the subtracted dispersion relations work much better than the unsubtracted ones. An exact dispersive representation for the form factors would include all possible inelasticities. In our framework we use only the two-pion inelasticity. Thus we neglect for instance the inelasticities caused by four pions, by a kaon-antikaon pair, by a baryon-antibaryon pair, ... In

practice these mesonic inelasticities start at $\sqrt{s} \approx 1\,\mathrm{GeV}$ and the baryonic ones at around $2\,\mathrm{GeV}$; see also the corresponding discussion in [31]. Thus, all these inelasticities except for the one caused by two pions are "high-energy inelasticities". If we limit ourselves to low values of q^2, then the influence of these high-energy inelasticities is suppressed by powers of $1/s$. The more subtractions one uses in the dispersive representation, the higher the suppression of the unaccounted high-energy inelasticities. Thus we have more trust in the subtracted dispersion relations (10) than in (11). If we found in practice a semi-quantitative agreement for the unsubtracted dispersion relations (12) and (13), then we would assume that the subtracted dispersion relations work well on a quantitative level. On the other hand, the subtracted dispersion relations are sufficient to deduce low-energy quantities like radii —(6), (7)— and curvatures. The general philosophy is that low-energy structures, *i.e.* variations in energy, are mainly caused by low-energy physics, the two-pion intermediate states.

In the dispersive formulae the quantity F_π^V denotes the pion form factor defined by

$$
\langle 0|j^\mu|\pi^+(p_+)\,\pi^-(p_-)\rangle = e\,(p_+^\mu - p_-^\mu)\, F_\pi^V((p_+ + p_-)^2).
$$
(14)

On account of (8) and (9) we consider the cases $\mu = 3, 1$. The corresponding difference of the pion momenta in (14) produces the angular dependence $\sim \cos\theta = d_{0,0}^1(\theta)$ for $\mu = 3$ and $\sim \sin\theta\cos\varphi = -d_{1,0}^1(\theta)\,(e^{i\varphi} + e^{-i\varphi})/\sqrt{2}$ for $\mu = 1$. Following [34] we have introduced Wigner's d-matrices; $d_{0,0}^1(\theta) = \cos\theta$ and $d_{1,0}^1(\theta) = -\sin\theta/\sqrt{2}$.

$T_{E/M}$ are the reduced amplitudes for the reaction $\Sigma^0\,\bar\Lambda \to \pi^+\pi^-$ projected on $J = 1$. We introduce them in two steps. We start with the general form of the reaction's invariant amplitude [34]

$$
\tilde{\mathcal{M}}(s,\theta,\varphi,\sigma,\lambda) = \\
\frac{1}{p_z} \sum_J \left(J + \frac{1}{2}\right) \phi^J(s; 0, 0, \sigma, \lambda)\, d_{(\sigma-\lambda),0}^J(\theta)\, e^{i(\sigma-\lambda)\varphi}\,,
$$
(15)

where $\phi^J(s; \lambda_c, \lambda_d, \lambda_a, \lambda_b)$ are Jacob/Wick helicity amplitudes for a reaction $a, b \to c, d$ with total angular momentum J and $d_{(\lambda_c-\lambda_d),(\lambda_a-\lambda_b)}^J(\theta)$ are the associated rotation matrices. For simplicity we also introduce

$$
\mathcal{M}(s,\theta,\sigma,\lambda) := \tilde{\mathcal{M}}(s,\theta,\varphi = 0,\sigma,\lambda).
$$
(16)

We are interested in $J = 1$. Using the orthogonal properties of the rotation matrices to invert (15) yields [34]

$$
\phi^1(s; 0, 0, \sigma, \lambda) = p_z \int_0^\pi \mathrm{d}\theta \sin\theta\, \mathcal{M}(s,\theta,\sigma,\lambda)\, d_{(\sigma-\lambda),0}^1(\theta).
$$
(17)

By comparison with the angular dependence emerging from the pion form factor we see that we have to focus on $d_{0,0}^1$ and $-d_{1,0}^1/\sqrt{2}$. Therefore we introduce the reduced amplitudes as

$$
T_E(s) := \frac{3}{2} \frac{\phi^1(s; 0, 0, +1/2, +1/2)}{\bar{v}_\Lambda(-p_z, +1/2)\gamma^3 u_\Sigma(p_z, +1/2) p_{\mathrm{c.m.}} p_z}\,,
$$
(18)

and

$$T_M(s) := -\frac{3}{2\sqrt{2}} \frac{\phi^1(s; 0, 0, +1/2, -1/2)}{\bar{v}_\Lambda(-p_z, -1/2)\, \gamma^1\, u_\Sigma(p_z, +1/2)\, p_{\text{c.m.}} p_z}. \tag{19}$$

$p_{\text{c.m.}}$ is the pion center-of-mass momentum. The reduced amplitudes are related to the general amplitudes by

$$\mathcal{M}(s, \theta, +1/2, +1/2) =$$
$$\bar{v}_\Lambda(-p_z, +1/2)\, \gamma^3\, u_\Sigma(p_z, +1/2)\, p_{\text{c.m.}}\, T_E(s)\, d_{0,0}^1(\theta)$$
$$+ \text{ other partial waves}, \quad J \neq 1, \tag{20}$$

and

$$\mathcal{M}(s, \theta, +1/2, -1/2) =$$
$$-\sqrt{2}\, \bar{v}_\Lambda(-p_z, -1/2)\, \gamma^1\, u_\Sigma(p_z, +1/2)\, p_{\text{c.m.}}\, T_M(s)\, d_{1,0}^1(\theta)$$
$$+ \text{ other partial waves}, \quad J \neq 1. \tag{21}$$

Finally (17) turns to

$$T_E(s) =$$
$$\frac{3}{2} \int_0^\pi \mathrm{d}\theta \sin\theta\, \frac{\mathcal{M}(s, \theta, +1/2, +1/2)}{\bar{v}_\Lambda(-p_z, +1/2)\gamma^3 u_\Sigma(p_z, +1/2)\, p_{\text{c.m.}}} \cos\theta \tag{22}$$

and

$$T_M(s) =$$
$$\frac{3}{4} \int_0^\pi \mathrm{d}\theta \sin\theta\, \frac{\mathcal{M}(s, \theta, +1/2, -1/2)}{\bar{v}_\Lambda(-p_z, -1/2)\, \gamma^1\, u_\Sigma(p_z, +1/2)\, p_{\text{c.m.}}} \sin\theta. \tag{23}$$

In practice these formulae are used for the bare input, not for the full amplitudes that contain pion rescattering.

Schematically the dispersion relation is depicted in fig. 1.

For the amplitude $T_{E/M}$ one should also consider pion rescattering encoded in the Omnès function

$$\Omega(s) = \exp\left\{ s \int_{4m_\pi^2}^\infty \frac{\mathrm{d}s'}{\pi} \frac{\delta(s')}{s'(s' - s - i\epsilon)} \right\} \approx F_\pi^V(s), \tag{24}$$

where δ denotes the pion p-wave phase shift [21,22]. This is depicted in fig. 2. In practice we will follow the recipe of [23] and parametrize the phase shift such that it smoothly reaches π at infinity. Contrary to [23] we do not include other inelasticities in the pion form factor, *i.e.* we do not distinguish between Ω and F_π^V. For our low-energy calculation this should not matter too much. Indeed we will see that other uncertainties are more severe.

The dispersive formalism used here assumes the absence of anomalous thresholds. They would appear if the left-hand cuts of the pion-hyperon amplitudes of figs. 1 and 2 contained poles for $s > 4m_\pi^2$. In turn this translates to masses m_{exch} that satisfy

$$m_{\text{exch}}^2 < \frac{1}{2}\left(m_\Sigma^2 + m_\Lambda^2 - 2m_\pi^2 \right). \tag{25}$$
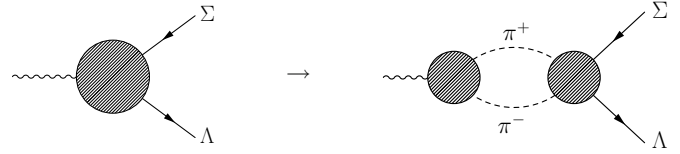
Fig. 1. The transition form factors are obtained from their two-pion inelasticity.
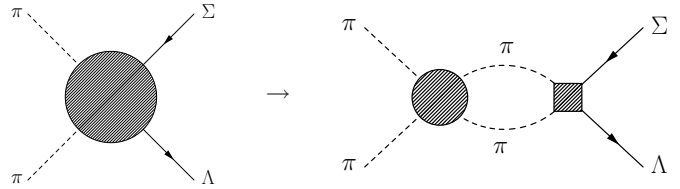
Fig. 2. The scattering amplitude is obtained from the two-pion rescattering and a part (box) containing only left-hand cuts and a polynomial.

The object with such a mass must have strangeness, baryon number and electric charge. The latter is required because neutral pions do not couple to photons because of the charge-conjugation symmetry of the strong and electromagnetic interaction. The lowest-mass state with strangeness, baryon number and charge is the single-particle state Σ^+ [1]. It violates the condition (25). This guarantees the absence of anomalous thresholds.

Along the lines of [28,33] one needs an approximation for the "bare" four-point amplitude K of $\Sigma^0 \bar{\Lambda} \to \pi^+ \pi^-$, where pion rescattering is ignored. In other words one needs the left-hand cuts of this amplitude. Ideally one would like to obtain this amplitude from (dispersion theory and) data from the crossed channel, *i.e.* from hyperon-pion scattering. Indeed, for the corresponding isovector part of the nucleon form factors such an analysis has been performed recently [31] based on a dispersive Roy-Steiner analysis of pion-nucleon scattering [36]. Since pions and hyperons are unstable, data on pion-hyperon scattering will not be available in the near future. For a coupled-channel analysis of pion-nucleon and kaon-nucleon scattering data with hyperons at least in the final states see [37]. We note in passing that strangeness channels are even important for pion-nucleon scattering: The dispersive Roy-Steiner analysis of pion-nucleon scattering [36] requires a coupled-channel analysis of pion-nucleon and kaon-nucleon scattering for the s-wave [38].

In lack of pion-hyperon scattering data we resort to the second best option and use in the following relativistic three-flavor χPT at next-to-leading order (NLO) to determine K. Strictly speaking the reaction amplitude for $\Sigma^0 \bar{\Lambda} \to \pi^+ \pi^-$ does not exist in baryon χPT, because there are no antibaryons in this framework. But the cross-channel amplitude $\Sigma^0 \pi^+ \to \Lambda \pi^+$ does exist and crossing symmetry and analytical continuation will provide the right answer.

Given any input for K, the scattering amplitude T is obtained by [28]

$$T(s) = K(s) + \Omega(s) P_{n-1}(s)$$
$$+ \Omega(s) s^n \int_{4m_\pi^2}^\infty \frac{ds'}{\pi} \frac{\sin\delta(s') K(s')}{|\Omega(s')| (s' - s - i\epsilon) s'^n} , \tag{26}$$

where P_{n-1} denotes a polynomial of degree $n-1$.

Note that any polynomial part of K can be put into P_{n-1} and need not be carried through the dispersion integral. Thus one can split up the calculated Feynman amplitudes into a part $\mathcal{M}^{\text{pole}}$ that contains the left-hand cuts —in practice they will emerge from the pole terms of u- and t-channel exchange diagrams— and a part $\mathcal{M}^{\text{contact}}$ that is purely polynomial. Recalling the projection formulae (22) and (23) this leads to

$$K_E(s) =$$
$$\frac{3}{2} \int_0^\pi d\theta \sin\theta \frac{\mathcal{M}^{\text{pole}}(s, \theta, +1/2, +1/2)}{\bar{v}_\Lambda(-p_z, +1/2) \gamma^3 u_\Sigma(p_z, +1/2) p_{\text{c.m.}}} \cos\theta \tag{27}$$

and

$$P_{n-1}^E(s) =$$
$$\frac{3}{2} \int_0^\pi d\theta \sin\theta \frac{\mathcal{M}^{\text{contact}}(s, \theta, +1/2, +1/2)}{\bar{v}_\Lambda(-p_z, +1/2) \gamma^3 u_\Sigma(p_z, +1/2) p_{\text{c.m.}}} \cos\theta \tag{28}$$

and the equivalent formulae for the magnetic part.

As already spelled out we will use three-flavor χPT to determine K and the polynomial P_{n-1}. Two versions are conceivable. One might or might not include the decuplet states explicitly. We will explore both options in the following. In any case we will restrict ourselves to NLO. As will be discussed below, leading order (LO) boils down to the exchange diagrams $\pi^+ \Sigma^0 \to \Sigma^+ \to \pi^+ \Lambda$ and (optionally) $\pi^+ \Sigma^0 \to \Sigma^{*+} \to \pi^+ \Lambda$ (s and u channel —or, concerning $\Sigma^0 \bar{\Lambda} \to \pi^+ \pi^-$, t and u channel). Here Σ^* denotes a decuplet state. The coupling constant of the latter can be adjusted to the measured decay widths $\Sigma^* \to \pi \Lambda$ or $\Sigma^* \to \pi \Sigma$; see further discussion below. NLO adds just contact terms (and provides the flavor splitting that leads to the physical masses of the states instead of one averaged mass per multiplet). If the decuplet states are not included explicitly, then the size of the NLO contact terms is modified such that the static version of the decuplet exchange is implicitly accounted for [39]. Loops appear only at next-to-next-to leading order (NNLO). They would bring in additional left-hand cuts. Our approximation for the input is depicted in fig. 3.

In formula (26) the pion loop starts to contribute when $\Omega(s)$ deviates from unity. This happens at order s. Therefore we cannot constrain the polynomial P_{n-1} better than to a constant, if our input is restricted to tree level, *i.e.* NLO of χPT. In other words we have to use $n = 1$ and drop all polynomial terms of higher order. We will see below that the Born terms produce a polynomial of order 0,
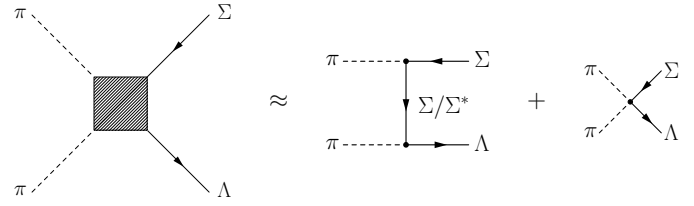
Fig. 3. The "bare" input (box) is obtained from NLO χPT.

i.e. a constant. For the magnetic/electric part the NLO contact term produces a polynomial of order 0/1 —see (50), (51) below. Thus one should keep the NLO contribution for the magnetic part, but not for the electric. All this is in line with the treatment of [8] as described in detail in Kubis' PhD Thesis [40] in the following sense. In a direct χPT calculation of the form factors the NLO contact term contributes only to the Pauli form factor F_2 [40]. On account of (2) the impact of F_2 on G_E relative to G_M is suppressed for low q^2.

As we will discuss below, the decuplet-exchange terms yield polynomials which depend on the spurious spin-1/2 contributions. For the electric part the ambiguity is of second chiral order which should be dropped anyway. For the magnetic part there is a constant term which can be accounted for equally well by the NLO contact term. Thus the polynomial part formally emerging from the decuplet exchange can be entirely dropped for the magnetic contribution. To obtain the proper low-energy limit of χPT we should use

$$P_0^E = P_{\text{Born}}^E + P_{\text{res}}^E,$$
$$P_0^M = P_{\text{Born}}^M + P_{\text{NLO } \chi\text{PT}}^M - K_{\text{res,low}}^M, \tag{29}$$

where the label "Born" denotes the Sigma exchange and "res" the exchange of the decuplet resonance. The label "NLO χPT" refers to χPT without the decuplet. $K_{\text{res,low}}^M$ denotes the low-energy limit of the resonance-pole contribution to the magnetic amplitude. A detailed analysis reveals that there are some subtleties with this low-energy limit due to the left-hand cut structure of the resonance-exchange contributions. This is discussed in detail in appendix B based on the results (54) below.

Note that the relation for the electric polynomial implies

$$P_{\text{res}}^E + K_{\text{res,low}}^E = \text{higher order} \tag{30}$$

to be consistent with the low-energy limit of χPT. We have checked that this is indeed the case.

Let us briefly discuss the convergence of the integrals in (10) and (26): If the pole terms from the Born diagrams (octet exchange) are projected on $J = 1$, they scale like $(\log s)/s$ for large s. The subtracted dispersion relation in (26) converges very well. The high-energy behavior of the curly bracket is then $\sim s^0$. Since the Omnès function behaves like $1/s$, the whole amplitude scales like $(\log s)/s$ at large s. This provides a very convergent integral in (10). The decuplet changes the picture to some extent: The pole terms diverge like $\log s$. Still this leads to convergent integrals.

On the other hand, the analytic structure of the scattering amplitudes $K_{M/E}$ changes where p_z or $p_{c.m.}$ have their zeros. This happens at $s_1 := (m_\Sigma - m_\Lambda)^2$, $s_2 := 4m_\pi^2$ and $s_3 := (m_\Sigma + m_\Lambda)^2$. We are interested in $q^2 < s_1$ for the transition form factors (10) and we try to obtain a reasonable approximation for the scattering amplitudes $K_{M/E}(s)$ and $T_{M/E}(s)$ in the low-energy part of $s_2 \le s < s_3$. Thus it does not make sense to evaluate the functions outside of $s_2 \le s < s_3$.

In practice we will terminate the integration range in (10) and in (26) by a finite cutoff Λ^2 and check the sensitivity of our results to a variation in Λ. From the previous considerations it is clear that we should keep the cutoff Λ below $\sqrt{s_3} = m_\Sigma + m_\Lambda$. We will vary Λ between 1 and 2 GeV and study the impact of this change on the results.

2.2 Lagrangians, parameters and input tree-level amplitudes

The relevant interaction part of the LO chiral Lagrangian [8] including only the octet baryons as active degrees of freedom is given by

$$\mathcal{L}_8^{(1)} = i\langle \bar{B}\gamma_\mu D^\mu B\rangle + \frac{D}{2}\langle \bar{B}\,\gamma^\mu\,\gamma_5\,\{u_\mu, B\}\rangle$$
$$+ \frac{F}{2}\langle \bar{B}\,\gamma^\mu\,\gamma_5\,[u_\mu, B]\rangle \qquad (31)$$

with the octet baryons collected in

$$B = \begin{pmatrix} \frac{1}{\sqrt{2}}\Sigma^0 + \frac{1}{\sqrt{6}}\Lambda & \Sigma^+ & p \\ \Sigma^- & -\frac{1}{\sqrt{2}}\Sigma^0 + \frac{1}{\sqrt{6}}\Lambda & n \\ \Xi^- & \Xi^0 & -\frac{2}{\sqrt{6}}\Lambda \end{pmatrix}, \qquad (32)$$

the Goldstone bosons encoded in

$$\Phi = \begin{pmatrix} \pi^0 + \frac{1}{\sqrt{3}}\eta & \sqrt{2}\,\pi^+ & \sqrt{2}\,K^+ \\ \sqrt{2}\,\pi^- & -\pi^0 + \frac{1}{\sqrt{3}}\eta & \sqrt{2}\,K^0 \\ \sqrt{2}\,K^- & \sqrt{2}\,\bar{K}^0 & -\frac{2}{\sqrt{3}}\eta \end{pmatrix}, \qquad (33)$$

$$u^2 := U := \exp(i\Phi/F_\pi), \qquad u_\mu := i\,u^\dagger(\nabla_\mu U)u^\dagger = u_\mu^\dagger, \qquad (34)$$

and $\langle \ldots \rangle$ denoting a flavor trace. The chirally covariant derivatives are defined by

$$D^\mu B := \partial^\mu B + [\Gamma^\mu, B] \qquad (35)$$

with

$$\Gamma_\mu := \frac{1}{2}\left(u^\dagger\,(\partial_\mu - i(v_\mu + a_\mu))\,u \right.$$
$$\left. + u\,(\partial_\mu - i(v_\mu - a_\mu))\,u^\dagger\right), \qquad (36)$$

and

$$\nabla^\mu U := \partial^\mu U - i(v^\mu + a^\mu)\,U + iU\,(v^\mu - a^\mu) \qquad (37)$$

where v and a denote external sources.

If one includes also the decuplet states as active degrees of freedom in χPT, then the relevant interaction part of the LO chiral Lagrangian reads [6, 19, 41]

$$\mathcal{L}_{8+10}^{(1)} = \mathcal{L}_8^{(1)}$$
$$+ \frac{1}{2\sqrt{2}}\,h_A\,\epsilon_{ade}\,g_{\mu\nu}\,(\bar{T}_{abc}^\mu\,u_{bd}^\nu\,B_{ce} + \bar{B}_{ec}\,u_{db}^\nu\,T_{abc}^\mu), \qquad (38)$$

where the decuplet is expressed by a totally symmetric flavor tensor T_{abc} with [19]

$$T_{111} = \Delta^{++}, \qquad T_{112} = \frac{1}{\sqrt{3}}\,\Delta^+,$$

$$T_{122} = \frac{1}{\sqrt{3}}\,\Delta^0, \qquad T_{222} = \Delta^-,$$

$$T_{113} = \frac{1}{\sqrt{3}}\,\Sigma^{*+}, \qquad T_{123} = \frac{1}{\sqrt{6}}\,\Sigma^{*0}, \qquad T_{223} = \frac{1}{\sqrt{3}}\,\Sigma^{*-},$$

$$T_{133} = \frac{1}{\sqrt{3}}\,\Xi^{*0}, \qquad T_{233} = \frac{1}{\sqrt{3}}\,\Xi^{*-}, \qquad T_{333} = \Omega. \qquad (39)$$

The last term in (38) provides the pion-hyperon three-point interactions. Of course, it is not unique how to write down this interaction term [6,18,19,37,39,42]. In principle, all differences can be encoded in the contact interactions that show up in χPT at NLO; see below. In practice, it might happen that different versions of the LO three-point interaction terms once used with physical masses induce flavor-breaking effects that are not entirely accounted for by NLO contact terms. From a formal point of view such effects are NNLO, but in practice it might matter to some extent; see also the discussion in [37]. In the present work we are not interested in a description of all hyperon form factors, but focus on the Σ^0-to-Λ transition. If one does not use or insist on cross-relations between NLO parameters induced by three-flavor symmetry, then all differences between different versions of the three-point interactions can be moved to the contact interactions. Below we will explore explicitly two versions of the LO three-point interaction term to substantiate our statements.

For the coupling constants we use $F_\pi = 92.4\,\mathrm{MeV}$, $D = 0.80$, $F = 0.46$ [8] and h_A determined from the partial decay width $\Sigma^* \to \pi\Lambda$ or $\Sigma^* \to \pi\Sigma$. The partial width for the decay of a decuplet state with mass M into an octet state with mass m plus a pion and with a coefficient c in the lagrangian of type (38) is given by

$$\Gamma = \frac{c^2}{12\pi}\,\tilde{p}_{c.m.}^3\,\frac{E_B + m}{M}, \qquad (40)$$

where $E_B = \sqrt{m^2 + \tilde{p}_{c.m.}^2}$ ($\tilde{p}_{c.m.}$) is the energy (momentum) of the outgoing baryon in the rest frame of the

decaying resonance. For the decays of interest one finds from the explicit interaction Lagrangian (38): $c_{\Sigma^* \Lambda \pi} = h_A/(2\sqrt{2}F_\pi)$, and $c_{\Sigma^* \Sigma \pi} = h_A/(2\sqrt{6}F_\pi)$. (Note that there are always two decay branches possible for each decay $\Sigma^* \to \Sigma\pi$.) Matching to the experimental results yields $h_A = 2.4$ from $\Sigma^* \to \Lambda\pi$ and h_A ranging between 2.2 and 2.3 from $\Sigma^* \to \Sigma\pi$ —here the mass differences between isospin partners matter! For the numerical calculations we will explore the range

$$h_A = 2.3 \pm 0.1. \tag{41}$$

We note in passing that one obtains a somewhat larger value for h_A from the partial decay width $\Delta \to N\pi$. Here $c_{\Delta N\pi} = h_A/(2F_\pi)$ and $h_A = 2.88$. Finally one might look at the large-N_c prediction (see, *e.g.*, [18, 43] and references therein — N_c denotes the number of colors): $h_A = 3g_A/\sqrt{2} = 2.67$ with $g_A = F + D = 1.26$. In the following we will use h_A for the vertices $\Sigma^* \Lambda\pi$ and $\Sigma^* \Sigma\pi$. Therefore we regard the determination from the Σ^* decays as the most reasonable ones for our purposes. The difference to the determination from the Δ decay points towards flavor breaking effects for this coupling which shows up at NNLO in the chiral counting.

According to [44] a complete and minimal NLO Lagrangian for the baryon-octet sector is given by

$$
\begin{aligned}
\mathcal{L}_8^{(2)} =\ & b_D \langle \bar{B}\{\chi_+, B\}\rangle + b_F \langle \bar{B}[\chi_+, B]\rangle + b_0 \langle \bar{B}B\rangle\langle\chi_+\rangle \\
& + b_1 \langle \bar{B}[u^\mu, [u_\mu, B]]\rangle + b_2 \langle \bar{B}\{u^\mu, \{u_\mu, B\}\}\rangle \\
& + b_3 \langle \bar{B}\{u^\mu, [u_\mu, B]\}\rangle + b_4 \langle \bar{B}B\rangle\langle u^\mu u_\mu\rangle \\
& + ib_5\big(\langle \bar{B}[u^\mu, [u^\nu, \gamma_\mu D_\nu B]]\rangle \\
& \quad - \langle \bar{B}\overleftarrow{D}_\nu[u^\mu, [u_\mu, \gamma_\mu B]]\rangle\big) \\
& + ib_6\big(\langle \bar{B}[u^\mu, \{u^\nu, \gamma_\mu D_\nu B\}]\rangle \\
& \quad - \langle \bar{B}\overleftarrow{D}_\nu\{u^\nu, [u^\mu, \gamma_\mu B]\}\rangle\big) \\
& + ib_7\big(\langle \bar{B}\{u^\mu, \{u^\nu, \gamma_\mu D_\nu B\}\}\rangle \\
& \quad - \langle \bar{B}\overleftarrow{D}_\nu\{u^\nu, \{u^\mu, \gamma_\mu B\}\}\rangle\big) \\
& + ib_8\big(\langle \bar{B}\gamma_\mu D_\nu B\rangle - \langle \bar{B}\overleftarrow{D}_\nu\gamma_\mu B\rangle\big)\langle u^\mu u^\nu\rangle \\
& + \frac{i}{2} b_9 \langle \bar{B}u^\mu\rangle\langle u^\nu \sigma_{\mu\nu}B\rangle \\
& + \frac{i}{2} b_{10} \langle \bar{B}\{[u^\mu, u^\nu], \sigma_{\mu\nu}B\}\rangle \\
& + \frac{i}{2} b_{11} \langle \bar{B}[[u^\mu, u^\nu], \sigma_{\mu\nu}B]\rangle \\
& + d_4\langle \bar{B}\{f_+^{\mu\nu}, \sigma_{\mu\nu}B\}\rangle + d_5\langle \bar{B}[f_+^{\mu\nu}, \sigma_{\mu\nu}B]\rangle \tag{42}
\end{aligned}
$$

with $\chi_\pm = u^\dagger \chi u^\dagger \pm u\chi^\dagger u$ and $\chi = 2B_0(s + ip)$ obtained from the scalar source s and the pseudoscalar source p. The low-energy constant B_0 is essentially the ratio of the light-quark condensate to the square of the pion-decay constant.

We note in passing that Frink and Meißner [45] agree with [44] at the NLO level displayed in (42), though not at NNLO. To be in line with the conventions of [8] we have re-labeled some of the coupling constants of [44]: $d_1 \to b_{10}/2$, $d_2 \to b_{11}/2$, $d_3 \to b_9/2$. The terms $\sim b_{D/F}$ provide the

mass splitting for the octet states. Concerning the interaction terms for $\bar{\Lambda}\Sigma^0\pi^+\pi^-$ only b_D, b_3, b_6, and b_{10} contribute. A more detailed investigation reveals that the b_6 term is not of NLO in this channel. Concerning the scattering of baryon-antibaryon to two pions the b_D, b_3 terms do not contribute to the p-wave. Thus for our p-wave amplitudes we will only need a value for b_{10}. If we do not include the decuplet states as explicit degrees of freedom, we can take the value of b_{10} from the corresponding works on χPT. In [39] a value of $b_{10} \approx 0.95\,\mathrm{GeV}^{-1}$ has been given. In [8] a somewhat larger value is used, $b_{10} \approx 1.24\,\mathrm{GeV}^{-1}$. In our calculations we will explore the range

$$b_{10} = (1.1 \pm 0.25)\,\mathrm{GeV}^{-1}. \tag{43}$$

In practice this is all we need to provide input for (29).

To illuminate the meaning and input for the contact interactions we add the following discussion. Unfortunately the value for b_{10} is not entirely based on experimental input. Instead a resonance saturation assumption enters the estimate for b_{10} [39]. In this framework a significant part of the value for b_{10} comes from the contribution of the decuplet exchange. Thus if the decuplet baryons are included as active degrees of freedom the low-energy constants in the NLO lagrangian must be readjusted. We denote the NLO low-energy constants of octet+decuplet χPT by $\tilde{b}_{...}$ instead of $b_{...}$. Consequently the relevant part of the NLO Lagrangian for octet+decuplet χPT is given by

$$\mathcal{L}_{8+10}^{(2)} = \mathcal{L}_8^{(2)}\Big|_{b_{...} \to \tilde{b}_{...}} + \text{mass splitting for decuplet.} \tag{44}$$

Note that this is not the complete NLO Lagrangian of octet+decuplet χPT, only the part relevant for our purposes.

As already stressed, the only NLO low-energy constant that really matters for our calculations is b_{10} or $\tilde{b}_{10}$, respectively. To relate these two quantities in the most reasonable way in view of the $\Sigma\Lambda\pi^+\pi^-$ amplitude we have to determine the low-energy and/or chiral-limit contribution to this amplitude from the decuplet exchange (see further discussion below). If we denote this contribution by b_{10}^{res} we have to choose $\tilde{b}_{10}$ such that the sum produces the result of pure baryon-octet χPT:

$$\tilde{b}_{10} + b_{10}^{\mathrm{res}} = b_{10}. \tag{45}$$

On the other hand, if we are not interested in an explicit value for $\tilde{b}_{10}$ we can just use (29).

Alternatively to the resonance saturation of [39] one might utilize input from [37]. There, scattering data on pion-nucleon and kaon-nucleon have been described by a chiral coupled-channel Bethe-Salpeter approach. In this framework the contact interactions have been determined from large-N_c constraints and fits to the scattering data. We have checked explicitly that these contact interactions can be translated to a b_{10} parameter that is in the range given in (43). Thus in practice we use (29) together with (43).

For the tree-level calculation of the four-point amplitude $\pi^+\pi^-\Sigma^0\bar{\Lambda}$ there can be exchange contributions from

the three-point vertices $\sim D, F, h_A$ and contact interactions from the NLO terms. In addition, one might get a contact term of Weinberg-Tomozawa type [46,47] from the chiralized kinetic term, i.e. from $\mathrm{tr}(\bar{B}\gamma^\mu[\Gamma_\mu, B])$. However, if one considers only pions, the non-trivial part of Γ_μ resides only in the first two rows and columns. There, however, the Λ part of B is proportional to the unit matrix. Therefore, the commutator $[\Gamma_\mu, B]$ vanishes and there is no Weinberg-Tomozawa term for the four-point amplitude we are interested in. (Considering $\bar{\Lambda}$ for $\bar{B}$ and Σ^0 for B does not change the argument, because one can shift the commutator to $\bar{B}$ within the flavor trace.)

The Feynman amplitude for the Born terms (exchange of octet $\Sigma^\pm$) is given by

$$\mathcal{M}_{\mathrm{Born}} =$$
$$\frac{D\,F}{\sqrt{3}F_\pi^2}\Bigg(\bar{v}_\Lambda u_\Sigma\, m_\Sigma\,(m_\Sigma^2 - m_\Lambda^2)\left(\frac{1}{t - m_\Sigma^2} - \frac{1}{u - m_\Sigma^2}\right)$$
$$+\bar{v}_\Lambda\gamma^\mu k_\mu u_\Sigma\, m_\Sigma\,(m_\Sigma + m_\Lambda)\left(\frac{1}{t - m_\Sigma^2} + \frac{1}{u - m_\Sigma^2}\right)$$
$$+\bar{v}_\Lambda\gamma^\mu k_\mu u_\Sigma\Bigg) \tag{46}$$

where $k = p_+ - p_-$ denotes the difference of the pion momenta and $t = (p_\Sigma - p_+)^2$. In the center-of-mass system we have $k = (0, 2\,p_{\mathrm{c.m.}}\sin\theta, 0, 2\,p_{\mathrm{c.m.}}\cos\theta)$. In line with (20), (21) we introduce reduced amplitudes. One obtains for the electric case, $\sigma = \lambda = +1/2$:

$$\frac{\mathcal{M}_{\mathrm{Born}}}{\bar{v}_\Lambda(-p_z, +1/2)\,\gamma^3\,u_\Sigma(p_z, +1/2)\,p_{\mathrm{c.m.}}} =$$
$$\frac{D\,F}{\sqrt{3}F_\pi^2}\Bigg(-\frac{s - (m_\Sigma + m_\Lambda)^2}{2\,p_{\mathrm{c.m.}}\,p_z}\,m_\Sigma\,(m_\Sigma - m_\Lambda)$$
$$\times\left(\frac{1}{t - m_\Sigma^2} - \frac{1}{u - m_\Sigma^2}\right)$$
$$-2\cos\theta\,m_\Sigma\,(m_\Sigma + m_\Lambda)\left(\frac{1}{t - m_\Sigma^2} + \frac{1}{u - m_\Sigma^2}\right)$$
$$-2\cos\theta\Bigg). \tag{47}$$

For the magnetic case, $\sigma = -\lambda = +1/2$, one finds

$$\frac{\mathcal{M}_{\mathrm{Born}}}{\bar{v}_\Lambda(-p_z, -1/2)\,\gamma^1\,u_\Sigma(p_z, +1/2)\,p_{\mathrm{c.m.}}} =$$
$$\frac{D\,F}{\sqrt{3}F_\pi^2}\Bigg(-2\sin\theta\,m_\Sigma(m_\Sigma + m_\Lambda)\left(\frac{1}{t - m_\Sigma^2} + \frac{1}{u - m_\Sigma^2}\right)$$
$$-2\sin\theta\Bigg). \tag{48}$$

Obviously we have pole terms and non-pole terms in (47) and (48). The respective p-wave projection is carried out by (22), (23). We denote the result for the pole terms by $K_{\mathrm{Born}}^{E/M}(s)$ and refrain from providing explicit expressions here. From (47), (48) one can immediately obtain

$$P_{\mathrm{Born}}^M = P_{\mathrm{Born}}^E = -2\,\frac{D\,F}{\sqrt{3}F_\pi^2}\,. \tag{49}$$

Note that the combination $\frac{1}{t-m_\Sigma^2} + \frac{1}{u-m_\Sigma^2}$ is a rational function in s, i.e. no square roots show up. Thus there is no problem with the analytical continuation of the amplitude below its nominal threshold $s = (m_\Sigma + m_\Lambda)^2$. The same holds true for the combination $\frac{1}{p_{\mathrm{c.m.}}\,p_z}\big(\frac{1}{t-m_\Sigma^2} - \frac{1}{u-m_\Sigma^2}\big)$. Concerning the analytic structure of the Born amplitudes in relation to electromagnetic form factors see also [48].

From the NLO Lagrangian (42) one obtains amplitudes $\sim \bar{v}_\Lambda u_\Sigma$ and $\sim \bar{v}_\Lambda i\sigma_{\mu\nu}u_\Sigma p_+^\mu p_-^\nu$. The first amplitude does not contribute to $J = 1$. The second one yields for the electric case, $\sigma = \lambda = +1/2$:

$$\bar{v}_\Lambda(-p_z, +1/2)i\sigma_{\mu\nu}u_\Sigma(p_z, +1/2)p_+^\mu p_-^\nu =$$
$$\bar{v}_\Lambda(-p_z, +1/2)\,\gamma^3\,u_\Sigma(p_z, +1/2)\,\frac{s\,p_{\mathrm{c.m.}}\cos\theta}{m_\Sigma + m_\Lambda}\,, \tag{50}$$

and for the magnetic case, $\sigma = -\lambda = +1/2$:

$$\bar{v}_\Lambda(-p_z, -1/2)i\sigma_{\mu\nu}u_\Sigma(p_z, +1/2)p_+^\mu p_-^\nu =$$
$$\bar{v}_\Lambda(-p_z, -1/2)\,\gamma^1\,u_\Sigma(p_z, +1/2)\,p_{\mathrm{c.m.}}\sin\theta\,(m_\Sigma + m_\Lambda). \tag{51}$$

The overall coupling constant and flavor factor that multiplies these expressions to obtain the Feynman amplitude is $+4b_{10}/(\sqrt{3}F_\pi^2)$.

As already spelled out, the electric part $\sim s$ is beyond our accuracy of NLO χPT. The magnetic part provides

$$P_{\mathrm{NLO}\,\chi\mathrm{PT}}^M = \frac{4b_{10}}{\sqrt{3}F_\pi^2}\,(m_\Sigma + m_\Lambda). \tag{52}$$

Working with relativistic spin-3/2 Rarita-Schwinger fields is plagued by ambiguities how to deal with the spurious spin-1/2 components. In the present context the interaction term $\sim h_A$ causes not only the proper exchange of spin-3/2 resonances, but induces an additional contact interaction. This unphysical contribution can be avoided by constructing interaction terms according to [18,42] or [49]. The Pascalutsa prescription boils down to the replacement [6,42]

$$T^\mu \to -\frac{1}{m_R}\,\epsilon^{\nu\mu\alpha\beta}\,\gamma_5\,\gamma_\nu\,\partial_\alpha T_\beta \tag{53}$$

where m_R denotes the resonance mass. Strictly speaking this procedure induces an explicit flavor breaking, but such effects are anyway beyond leading order. In practice, we take the (average) mass of the Σ^* resonance, $m_R := m_{\Sigma^*} \approx 1.385\,\mathrm{GeV}$.

The spurious spin-1/2 components can only provide contact terms, i.e. polynomial terms, which do not have a left-hand cut. Therefore they are completely irrelevant, if the polynomial part of the amplitude is determined anyway by matching the expression (26) to χPT. This is the essence of (29). We will perform calculations with both interaction terms, the "naive" one given in (38) and the "consistent" interaction obtained by (53). We will see that the pole terms remain unchanged.

Using the "naive" interaction term from (38) the contributions from the exchange of Σ^* decuplet baryon resonances are given by

$$
\begin{aligned}
\mathcal{M}_{\text{res}}^{\text{n}} = \frac{h_A^2}{8\sqrt{3}F_\pi^2} \Bigg(& \bar{v}_\Lambda u_\Sigma \, \frac{m_\Sigma + m_\Lambda}{12 m_{\Sigma^*}^2} (t-u) \\
& - \bar{v}_\Lambda u_\Sigma \, F(s) \left(\frac{1}{t-m_{\Sigma^*}^2} - \frac{1}{u-m_{\Sigma^*}^2} \right) \\
& + \bar{v}_\Lambda \gamma^\mu k_\mu u_\Sigma \frac{1}{12 m_{\Sigma^*}^2} \left(-2m_{\Sigma^*}^2 - 2m_{\Sigma^*}(m_\Sigma + m_\Lambda) \right. \\
& \left. + m_\Sigma^2 + m_\Lambda^2 + s - 6m_\pi^2 \right) \\
& + \bar{v}_\Lambda \gamma^\mu k_\mu u_\Sigma \frac{1}{2} G(s) \left(\frac{1}{t-m_{\Sigma^*}^2} + \frac{1}{u-m_{\Sigma^*}^2} \right) \Bigg)
\end{aligned}
\tag{54}
$$

with

$$
\begin{aligned}
F(s) := & \left(\frac{m_\Sigma + m_\Lambda}{2} + m_{\Sigma^*} \right) H_1(s) \\
& + \left(\frac{m_\Sigma + m_\Lambda}{2} - m_{\Sigma^*} \right) H_2,
\end{aligned}
\tag{55}
$$

$$
G(s) := H_1(s) + H_2,
\tag{56}
$$

$$
\begin{aligned}
H_1(s) := & \frac{m_\Sigma^2 + m_\Lambda^2 - s}{2} \\
& - \frac{(m_\Lambda^2 + m_{\Sigma^*}^2 - m_\pi^2)(m_\Sigma^2 + m_{\Sigma^*}^2 - m_\pi^2)}{4 m_{\Sigma^*}^2},
\end{aligned}
$$

$$
\begin{aligned}
H_2 := & \frac{1}{3} \left(m_\Lambda + \frac{m_\Lambda^2 + m_{\Sigma^*}^2 - m_\pi^2}{2 m_{\Sigma^*}} \right) \\
& \times \left(m_\Sigma + \frac{m_\Sigma^2 + m_{\Sigma^*}^2 - m_\pi^2}{2 m_{\Sigma^*}} \right).
\end{aligned}
\tag{57}
$$

As a cross-check for our calculations we have calculated the nucleon- and Delta-exchange contributions to $p\bar{n} \to \pi^+\pi^0$. They are related by large-N_c relations; see appendix A.

Only the contact terms change if one uses the "consistent" Pascalutsa interaction obtained by (53)

$$
\begin{aligned}
\mathcal{M}_{\text{res}}^{\text{P}} = \frac{h_A^2}{8\sqrt{3}F_\pi^2} \Bigg(& \bar{v}_\Lambda u_\Sigma \, \frac{4m_{\Sigma^*} + 3m_\Sigma + 3m_\Lambda}{12 m_{\Sigma^*}^2} (t-u) \\
& - \bar{v}_\Lambda u_\Sigma \, F(s) \left(\frac{1}{t-m_{\Sigma^*}^2} - \frac{1}{u-m_{\Sigma^*}^2} \right) \\
& + \bar{v}_\Lambda \gamma^\mu k_\mu u_\Sigma \frac{1}{12 m_{\Sigma^*}^2} \\
& \times \left(-2m_{\Sigma^*}^2 + 2m_{\Sigma^*}(m_\Sigma + m_\Lambda) + 3m_\Sigma^2 + 3m_\Lambda^2 \right. \\
& \left. + 4m_\Sigma m_\Lambda - 5s + 2m_\pi^2 \right) \\
& + \bar{v}_\Lambda \gamma^\mu k_\mu u_\Sigma \frac{1}{2} G(s) \left(\frac{1}{t-m_{\Sigma^*}^2} + \frac{1}{u-m_{\Sigma^*}^2} \right) \Bigg).
\end{aligned}
\tag{58}
$$

We see that in (54) and (58) the pole terms agree for both prescriptions. We use these pole terms to obtain $K_{\text{res}}^{E/M}(s)$.

The polynomial contribution to the electric amplitude is given by

$$
\begin{aligned}
P_{\text{res}}^E = & \frac{h_A^2}{24\sqrt{3}F_\pi^2 \, m_{\Sigma^*}^2} \\
& \times (m_{\Sigma^*}^2 + m_{\Sigma^*}(m_\Sigma + m_\Lambda) + m_\Sigma m_\Lambda) \\
& + \mathcal{O}(m_\pi^2, s).
\end{aligned}
\tag{59}
$$

Only the subleading parts $\sim m_\pi^2, s$ are different for (54) and (58). We will neglect them in the following and just use:

$$
\begin{aligned}
P_{\text{res}}^E \approx & \frac{h_A^2}{24\sqrt{3}F_\pi^2 \, m_{\Sigma^*}^2} \\
& \times (m_{\Sigma^*}^2 + m_{\Sigma^*}(m_\Sigma + m_\Lambda) + m_\Sigma m_\Lambda).
\end{aligned}
\tag{60}
$$

Finally we need the low-energy limit of $K_{\text{res}}^M(s)$ for the matching procedure spelled out in eq. (29). Due to the left-hand cut structure of this amplitude there are some subtleties with this low-energy limit. This is discussed in detail in appendix B. The result of these considerations is

$$
\begin{aligned}
K_{\text{res,low}}^M = & \frac{h_A^2}{24\sqrt{3}F_\pi^2} \\
& \times \frac{(-m_{\Sigma^*}^2 + 4m_{\Sigma^*}m_\Sigma - m_\Sigma^2)(m_{\Sigma^*} + m_\Sigma)}{m_{\Sigma^*}^2 (m_{\Sigma^*} - m_\Sigma)}.
\end{aligned}
\tag{61}
$$

The formulae (49), (52), (60), (61) together with

$$
K^{E/M}(s) = K_{\text{Born}}^{E/M}(s) + K_{\text{res}}^{E/M}(s)
\tag{62}
$$

fully determine the input for (26), (29). Starting conceptually from octet χPT one can study the successive approximations of using a) "Born": only the Born terms, b) "NLO": Born plus NLO contact terms, and finally c) "NLO+res": the impact of including explicitly the decuplet exchange. Note that for the electric case there are no NLO corrections. Here we study "Born" and the addition of resonances. To avoid a clutter of expressions we call the latter option also "NLO+res".
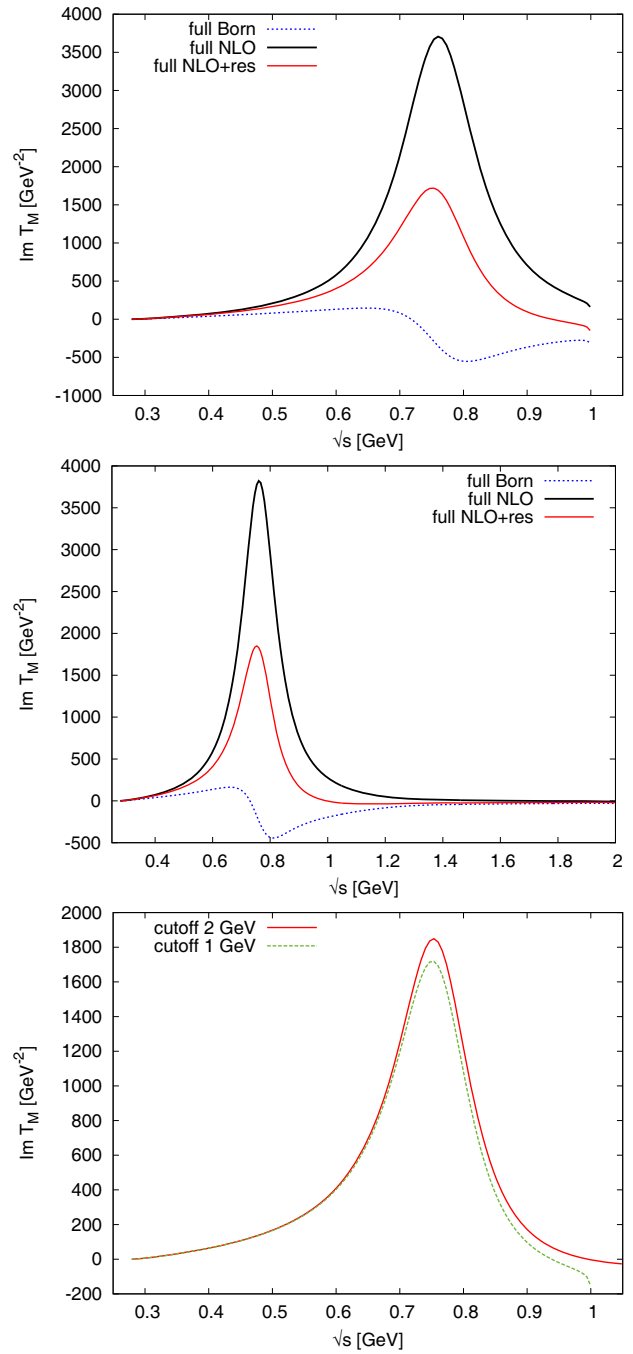
3 Results

As a first step we fix the input parameters to the central values given in (41) and (43), respectively. We address mainly two questions: How important is the exchange of decuplet resonances if their static part is already taken into account by NLO χPT? How strongly do the results depend on the cutoff Λ? We will show results for Λ equal to 1 and 2 GeV, respectively.

Figures 4–7 show real and imaginary part of the formal (sub-threshold) electric and magnetic scattering amplitudes. Obviously the pion rescattering drastically reshapes the amplitudes providing the expected structure around the rho meson. Only at very low energies the impact of pion rescattering is negligible. From the magnetic
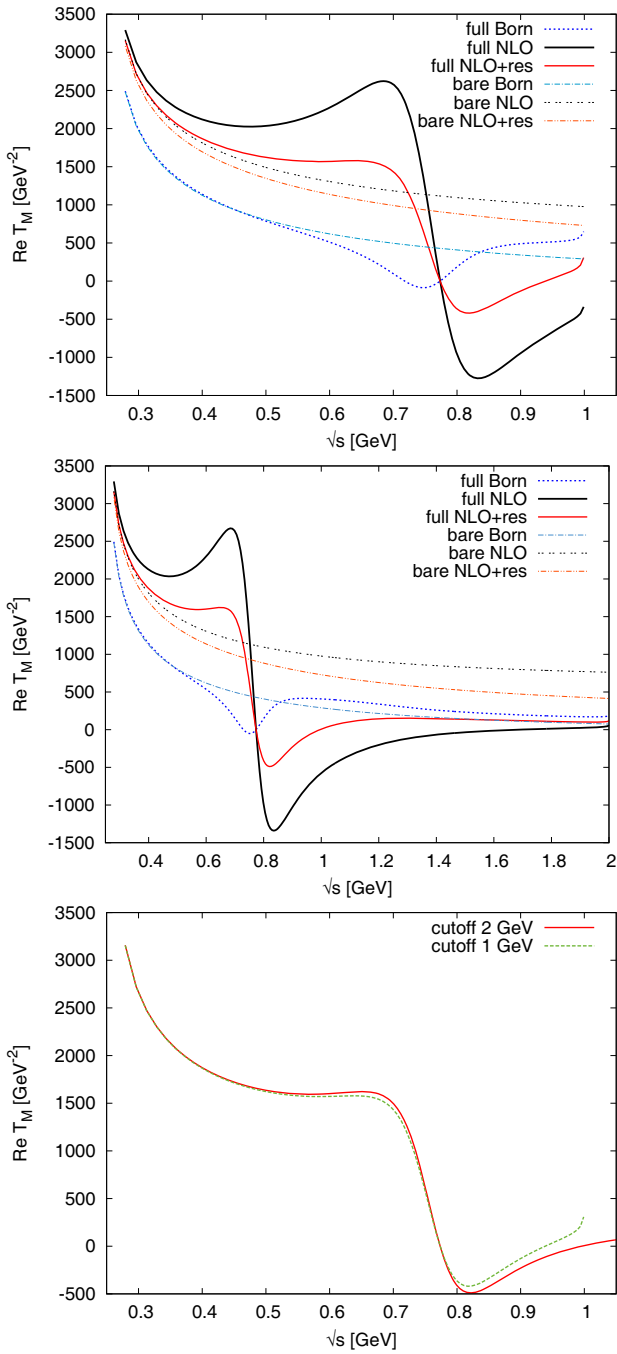
Fig. 4. Real part of the magnetic scattering amplitude. Top: $\Lambda = 1\,\text{GeV}$; middle: $\Lambda = 2\,\text{GeV}$; bottom: Comparison of the complete result ("NLO+res") for the two values of the cutoff Λ. The label "bare" denotes the input amplitude K, the label "full" the amplitude including pion rescattering. For the non-color version we spell out the ordering of curves as they start out from the left. In the top and middle panel from top to bottom one has 1. "full NLO", 2. "full NLO+res", 3. "bare NLO", 4. "bare NLO+res", 5. "bare Born", 6. "full Born".

Fig. 5. Imaginary part of the magnetic scattering amplitude. For the non-color version we spell out the ordering of curves. In the top and middle panel from top to bottom one has 1. "full NLO", 2. "full NLO+res", 3. "full Born". Note that the bare amplitudes have no imaginary part in the displayed region. See the caption of fig. 4 for more details.

sector we observe that the NLO term qualitatively changes all the results as compared to the pure Born terms. The explicit resonance terms do not change the qualitative picture any more,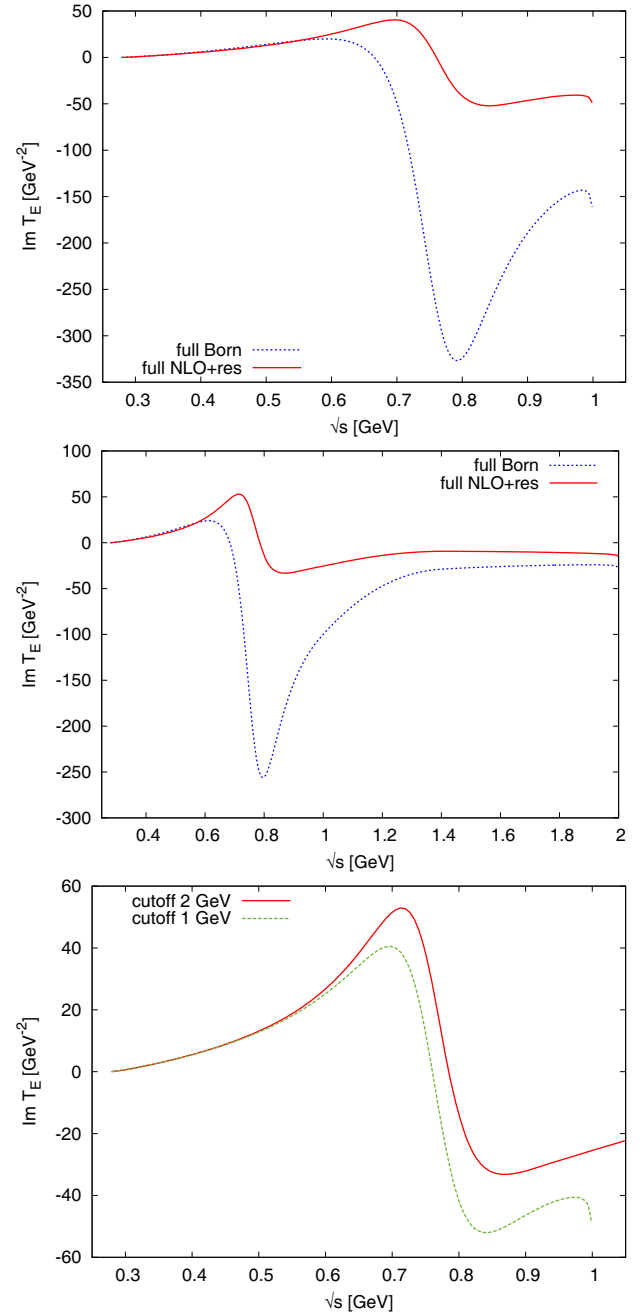 but "damp" to some extent the structures emerging at NLO. In the electric sector we observe also that the resonances matter. The impact of the variation in the cutoff, however, is in general rather small. This is very satisfying given that a χPT input loses its validity at higher energies.

From studying the scattering amplitudes alone one cannot tell easily how strongly the form factors are
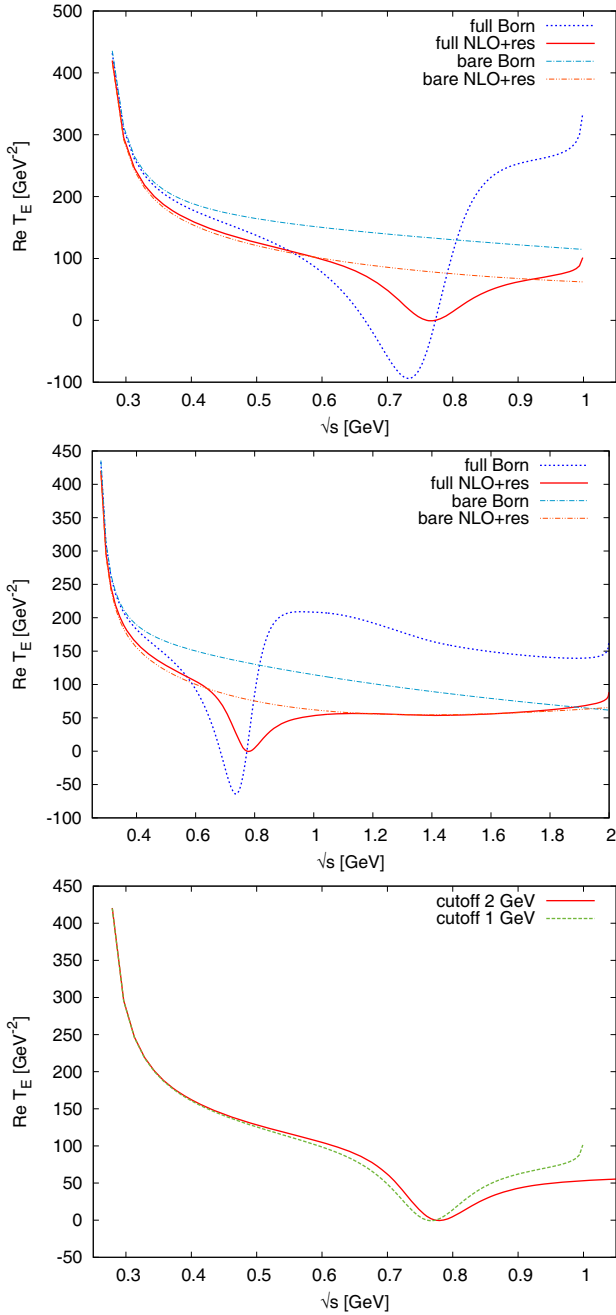
Fig. 6. Real part of the electric scattering amplitude. For the non-color version we spell out the ordering of curves as they start out from the left. In the top and middle panel from top to bottom one has 1. "bare Born", 2. "full Born", 3. "full NLO+res", 4. "bare NLO+res". See the caption of fig. 4 for more details.

Fig. 7. Imaginary part of the electric scattering amplitude. See the caption of fig. 4 for more details.

influenced. Table 1 documents the results from the unsubtracted dispersion relations (12) and (13) for the multipole moments and from the subtracted dispersion relations (10) for the radii (6), (7) using the central values of h_A and b_{10}. In general one observes that the Born terms alone are insufficient to produce reasonable results. The inclusion of the NLO term and/or the decuplet-resonance exchange improves the picture significantly —signs and orders of

magnitude come out correctly. Interestingly even the unsubtracted dispersion relations produce quite reasonable results. In particular in the electric sector the resonance exchange has the potential to cancel the Born contribution such that essentially the vanishing of the electric charge is achieved. In most of the cases varying the cutoff provides changes on the level of 10% at most. Thus the dispersive representation is most sensitive to the low-energy regime. This is an encouraging result given the χPT input and the fact that not considered inelasticities like four-pion states effectively come into play at around 1 GeV [27].

Table 1. Comparison to χPT [8] using $h_A = 2.3$, $b_{10} = 1.1\,\mathrm{GeV}^{-1}$.

Λ [GeV]	Quantity	Born	NLO	NLO+res	χPT
1	$G_M(0)$	-0.438	5.55	2.58	1.98 (exp.)
2		-0.65	5.98	2.66	
1	$\langle r_M^2 \rangle$ [GeV^{-2}]	0.453	33.7	17.9	18.6
2		0.613	35.2	18.8	
1	$G_E(0)$	-0.432	–	0.0026	0
2		-0.562	–	-0.031	
1	$\langle r_E^2 \rangle$ [GeV^{-2}]	-3.13	–	0.866	0.773
2		-2.91	–	1.044	

Table 2. Comparison to χPT [8] using $\Lambda = 2\,\mathrm{GeV}$, $h_A = 2.3$ and varying the value for b_{10} (in units of GeV^{-1}).

b_{10}	Quantity	NLO	NLO+res	χPT
0.85	$G_M(0)$	4.47	1.15	1.98 (exp.)
1.35		7.49	4.17	
0.85	$\langle r_M^2 \rangle$ [GeV^{-2}]	27.4	10.9	18.6
1.35		43.1	26.7	

Table 3. Comparison of the full calculation "NLO+res" to χPT [8] using $\Lambda = 2\,\mathrm{GeV}$, $b_{10} = 1.1\,\mathrm{GeV}^{-1}$ and varying the value for h_A.

Quantity	$h_A = 2.2$	$h_A = 2.4$	χPT
$G_M(0)$	2.94	2.36	1.98 (exp.)
$\langle r_M^2 \rangle$ [GeV^{-2}]	20.2	17.3	18.6
$G_E(0)$	-0.076	0.016	0
$\langle r_E^2 \rangle$ [GeV^{-2}]	0.708	1.40	0.773

Table 4. Comparison to χPT [8] using $\Lambda = 2\,\mathrm{GeV}$, $h_A = 2.22$, $b_{10} = 1.06\,\mathrm{GeV}^{-1}$.

Quantity	Born	NLO	NLO+res	χPT
$G_M(0)$	-0.648	5.74	2.65	1.98 (exp.)
$\langle r_M^2 \rangle$ [GeV^{-2}]	0.613	34.0	18.7	18.6
$G_E(0)$	-0.562	–	-0.068	0
$\langle r_E^2 \rangle$ [GeV^{-2}]	-2.907	–	0.774	0.773

After having convinced ourselves that the variation of the cutoff produces only moderate changes we keep $\Lambda = 2\,\mathrm{GeV}$ fixed and explore the impact of variations of the other two input parameters. In table 2 we explore the changes of the low-energy quantities if the value of b_{10} is varied according to (43). Since the electric sector is independent of b_{10} we restrict ourselves to the magnetic quantities. The conclusions to be drawn from inspecting table 2 are: One needs the decuplet, only then one obtains reasonable values for the magnetic radius. Interestingly even the unsubtracted dispersion relation works not too badly. However, the uncertainty related to b_{10} is sizable. Results change by a factor of 2 or more. Clearly a much better knowledge of b_{10} is mandatory to improve on the predictions in the magnetic sector.

Table 3 displays the consequences of the variation in h_A according to (41). In the magnetic sector the changes caused by variations in h_A are moderate. Thus once one has achieved a better handle on b_{10}, then satisfying predictive power for the magnetic sector can be achieved. In

other words, a measurement of the magnetic transition radius, *e.g.* at FAIR, would pin down b_{10} and drastically decrease the uncertainties of the low-energy magnetic transition form factor.

The electric sector is independent of b_{10}. Table 3 shows that for reasonable values of h_A the value of $G_E(0)$ can even be fine-tuned to zero. The smallness of the electric radius as predicted in [8] is qualitatively reproduced.

Obviously by just tuning the parameters in reasonable ranges all electric and magnetic low-energy quantities can be reproduced —not all at the same time, but one would not expect the unsubtracted dispersion relations to hold exactly. To illustrate this further we tune h_A and b_{10} such that the electric and magnetic radii are essentially reproduced. The results are shown in table 4. In particular we needed only a little change in h_A to fine-tune the comparatively rather small electric radius. The point here is that the Born and resonance exchange contributions nearly cancel each other as can be seen from the comparison of the pure Born and the complete result for the electric radius in both tables 1 and 4. We note in passing that this is qualitatively in line with the large-N_c considerations discussed in appendix A.

We will not explore at all the impact of a variation of the other input on our calculations. The parameters F and D are better constrained than h_A. Given our quite sizable uncertainties there is no point in exploring in this first paper the consequences from the differences in the pion phase shift as provided in [22] or [21], respectively. For the results we have utilized the phase shift from [22]. The same remark applies to the differences between the
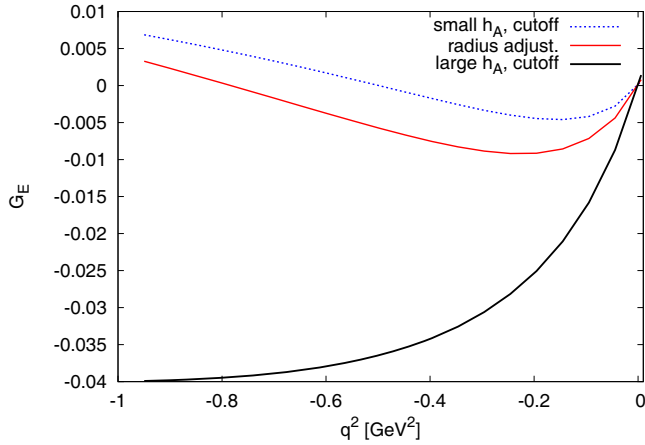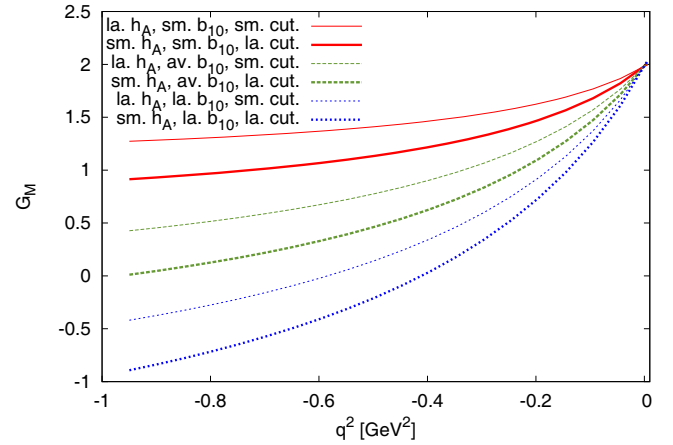
Fig. 8. The electric transition form factor obtained from the subtracted dispersion relation (10). The curve labeled by "radius adjust." is obtained with the parameter values of table 4. The label "small/large h_A, cutoff" refers to the lower/upper value of the range (41) and to $\Lambda = 1/2\,\text{GeV}$. See main text for details. For the non-color version we spell out the ordering of curves. In the space-like region one has from top to bottom the same ordering as in the legend.

Fig. 9. The magnetic transition form factor obtained from the subtracted dispersion relations (10). The label "sm./la. h_A" refers to the lower/upper value of the range (41). The label "sm./av./la. b_{10}" refers to the lower/medium/upper value of the range (43). The label "sm./la. cut." refers to $\Lambda = 1/2\,\text{GeV}$. For the non-color version we spell out the ordering of curves. In the space-like region one has from top to bottom the same ordering as in the legend.

pion form factor and the Omnès function at larger energies [23]. All these uncertainties can be explored if the parameters b_{10} and h_A are better under control and/or if a χPT calculation for the hyperon-pion amplitudes beyond NLO is used.

We use the subtracted dispersion relations (10) to determine the form factors in the region $q^2 < (m_\Sigma - m_\Lambda)^2$. The electric transition form factor is shown in fig. 8. By varying h_A in the range (41) and the cutoff Λ between 1 and 2 GeV we created a family of curves. In fig. 8 we show the respective highest and lowest curve. In addition we show the curve determined with the parameter values of table 4, which have been adjusted to the central value of the electric radius as obtained in [8]. The main conclusion from fig. 8 is that the electric transition form factor remains quite small over a large range of q^2. This is somewhat different from the result of [8] where a larger curvature and therefore a larger variation with q^2 has been found. Note, however, that this curvature is not obtained from pure χPT but from introducing an additional Lagrangian for vector mesons into the framework. Naturally this is associated with some model uncertainties that are hard to quantify. In our approach the ρ-meson — the only relevant vector meson in the isovector channel— is included by dispersion theory. On the other hand, given the restriction of our χPT input to NLO, we do not want to claim that we have our uncertainties fully under control. But the results from tables 1–4 are encouraging.

The magnetic transition form factor is presented in fig. 9. Concerning the variation in h_A and Λ we show again only the curves that encompass the whole respective family of curves. Obviously the value for b_{10} has the largest impact on the magnetic transition form factor. A better knowledge of b_{10} would significantly decrease the uncertainty.

4 Further discussion, summary and outlook

It is worth to compare a direct χPT calculation to our framework, which combines dispersion theory with purely hadronic χPT. A relativistic χPT calculation up to (including) order Q^4, *i.e.* a full one-loop calculation, has been presented in [8,40]. Our dispersive approach includes automatically all the χPT one-loop diagrams where the virtual photon couples to the pion. However, it does not include the loop diagrams where the photon couples to kaons or baryons. On the other hand, from the point of view of a dispersive representation the contribution of the diagrams with the coupling of the photon to kaons or baryons is suppressed at low energies, in particular for a subtracted dispersion relation. Thus, such diagrams might contribute to the absolute size of a form factor, but not much to the energy variation of the form factor. Therefore we expect that using the experimental values for the form factors at the photon point but extracting radii and general shape from the (subtracted) dispersive representation should effectively include the dominant physics contained in a one-loop χPT calculation. Dispersion theory goes even beyond one-loop by including pion rescattering to all orders. Thus the dynamical effects of the ρ-meson are automatically included, not only in a static approximation via low-energy constants or by adding a vector-meson lagrangian to χPT, which induced to some extent a model dependence. Of course, one future improvement of the present formalism could be to include the kaon-antikaon inelasticity and explore its impact on the shape of the form factors. Strictly speaking one should also include on the same footing the four-pion inelasticity, but maybe the corresponding three-loop diagrams are less important.

There is a second aspect where our combined framework might be superior to a pure χPT calculation. There

the decuplet states are not included as active degrees of freedom since they are not degenerate with the octet in the chiral limit. The decuplet appears indirectly in a static version by influencing the low-energy constants. Our results suggest that the explicit inclusion of dynamical decuplet states might be important, qualitatively in line with, e.g., [6, 18, 19, 37]. Of course, the inclusion of a dynamical decuplet can also be performed in a χPT framework, but the whole development is in an infant stage. Not even the full NLO lagrangian for relativistic three-flavor octet+decuplet baryon χPT has been formulated up to now. This deficiency will also concern our framework when we will apply it to the decuplet-to-octet transition form factors. For the present work, where the external states are octet hyperons, the inclusion of the decuplet intermediate states was very straightforward. Since the pionic loops are generated by the dispersive representation and not by an explicit loop calculation, there is no ambiguity related to the renormalization of the loop diagrams [6, 8, 17–19, 37].

For our hadronic input for the pion-hyperon scattering amplitudes we have used the language of three-flavor χPT. Conceptually this seems to be at odds with our dispersive setup where we include only the pions as intermediate states and not also the kaons. As already pointed out the influence of the kaon inelasticity starts at rather high energies, $(2m_K)^2 \approx 1\,\text{GeV}^2$. In principle, we could have formulated our whole framework in a language with two light flavors. There, pions would couple to the isosinglet Λ and the isotriplet Σ and Σ^* states. Without the notion of a three-flavor chiral limit the mass difference between Λ and Σ would not vanish, but one can assume nonetheless that the mass difference is a small quantity —similar in spirit to the assumption that the mass difference between Σ and Σ^* constitutes another small quantity, which does not vanish in the chiral limit. In such a framework the coupling constants for Σ^*-Λ-π and Σ^*-Σ-π would be independent from each other. But both can be determined from the Σ^* partial decay widths. This is what we essentially did anyway. In this framework with two light flavors those coupling constants would be independent of the Δ-N-π coupling constant. For our numerics we did not use such a three-flavor relation. The only input that we used from a three-flavor analysis are the values for D and F, i.e. the coupling constants for Σ-Λ-π and Σ-Σ-π, respectively. In a two-flavor framework these constants would not be related to g_A, i.e. to the N-N-π coupling constant. In our present analysis we use D and F just as input. Of course, their sizes are determined from a three-flavor formalism, but the flavor breaking is relatively well explored here. In summary, to a large extent our whole approach can be formulated in a language with two light flavors. Conceptually this connects our present work to the electromagnetic form factors of the charmed Λ_c, Σ_c, Σ_c^* states[4] [1]. We do not dwell on this connection any further in the present work.

Let us now summarize our results: In the electric sector we have found that the inclusion of the decuplet Σ^*

resonances is crucial. This leads to a large cancelation between Σ and Σ^* exchange such that even the unsubtracted dispersion relation for the electric transition form factor is reasonably satisfied. The cancelation leads to a small electric transition radius, in qualitative agreement with the direct three-flavor χPT calculation [8]. Even quantitative agreement can be achieved by a fine-tuning of the coupling constant that governs the decay width of the Σ^* resonances.

The inclusion of the decuplet for the calculation of the electric radii has also been discussed in [50] in the heavy-baryon limit of χPT. There the decuplet did not contribute to the Σ-Λ transition radius. Obviously this is different in our relativistic set-up.

As a further consequence of the cancelation between Σ and Σ^* exchange our electric transition form factor remains small throughout the whole low-energy region. This does not fully agree with the results of [8] obtained in a framework where three-flavor χPT is augmented with explicit vector-meson fields in the antisymmetric tensor representation. We would like to stress again that the inclusion of vector mesons in χPT is not an entirely model-independent procedure —one of the reasons why we replace this part of the framework by dispersion theory. Clearly it remains to be seen how the electric transition form factor is modified, if the hadronic input is pushed to higher orders and/or the kaon inelasticity is included.

The magnetic sector is sensitive to a low-energy constant of NLO χPT. Without the inclusion of such a term there remains an ambiguity how to properly treat the spin-3/2 Σ^* resonances in a relativistic framework (in the electric sector this ambiguity is relegated to NNLO). With a reasonable size estimate for this low-energy constant we can reproduce the three-flavor χPT prediction [8] for the magnetic transition radius. In turn by a measurement of the magnetic transition radius this low-energy constant could be narrowed down, leading to a significant increase of predictive power for the low-energy shape of the magnetic transition form factor. Such a measurement could be feasible at FAIR by determining the differential decay width of $\Sigma^0 \to \Lambda\, e^+ e^-$. In general, this Dalitz decay depends on two variables, for instance the dilepton mass and the angle between Λ and electron in the dilepton rest frame [12]. However, if the electric transition radius is small —as suggested by our results and the ones from [8]—, then a decay width that is just one-fold differential in the dilepton invariant mass would be sufficient to extract the magnetic transition radius. A back-to-the-envelope estimate shows that the effort to extract a magnetic transition radius from $\Sigma^0 \to \Lambda\, e^+ e^-$ is comparable to the extraction of the slope of the pion transition form factor from $\pi^0 \to \gamma\, e^+ e^-$; see [51] for a recent experiment and [52] for a recent dispersive calculation.

The framework presented here can be extended to all isovector form factors and transition form factors of the spin-1/2 and spin-3/2 baryon ground states. For the octet and decuplet states one might use the very same three-flavor chiral input for the baryonic scattering amplitudes. This might provide some additional cross-relations between observables that we have not utilized so far with our

---

[4] We thank M.F.M. Lutz for pointing out this interesting cross-relation.

focus on just the one transition from Σ^0 to Λ. On the other hand, if one wants to be more conservative, one might just use isospin symmetry and a two-flavor chiral input separately for each strangeness sector. The complementary experimental program would be a dedicated study of the differential distributions of hyperon Dalitz decays $Y \to Y' e^+ e^-$. With data input and dispersion theory the experimentally hardly accessible space-like region can be addressed, which in turn could provide a new angle on the structure of baryons.

Additional remark: Meanwhile an extended version of [53] appeared as a preprint [54]. All hyperons are addressed there while we focus here on the transition of Σ^0 to Λ. Leading-order chiral perturbation theory (with the inclusion of the decuplet) is used in [54] while we include the next-to-leading-order terms. In addition we include pion rescattering for the hyperon-pion scattering amplitudes via (26). Essentially the approach of [54] is recovered from (26) by first dropping the terms with K and then replacing the polynomial by the complete leading-order expression for the scattering amplitude that contains the polynomial and the left-hand-cut parts.

Appendix A. Cross-check with Δ exchange and large-N_c relations

As a cross-check of the results (46), (54) we have also calculated the nucleon- and Delta-exchange contributions to $p\bar{n} \to \pi^+\pi^0$. The nucleon exchange is obtained from (46) by replacing all the hyperon masses by the nucleon mass m_N and by

$$\frac{DF}{\sqrt{3}} \to -\frac{\sqrt{2}\,g_A^2}{4}. \tag{A.1}$$

The Delta exchange is obtained from (54) by replacing the hyperon masses by m_N, the Σ^* mass by m_Δ and

$$-\frac{h_A^2}{\sqrt{3}} \to \frac{2\sqrt{2}\,h_A^2}{3}. \tag{A.2}$$

In the large-N_c limit the leading-order contributions to the electric amplitude from nucleon exchange and Delta exchange should cancel each other. The nucleon-exchange contribution to the magnetic amplitude should be twice the one from Delta exchange (here with same sign); see, *e.g.*, the corresponding discussion in [55] and references therein.

This is indeed what one finds. We first note that the nucleon exchange does not contain the structure $\bar{v}_n u_p$. Therefore one obtains $T_M^N = T_E^N$. For both the nucleon and the Delta exchange the pole terms dominate the polynomial terms in the large-N_c limit. This is satisfying as the polynomial terms for the Delta exchange depend on the spurious spin-$1/2$ modes. In the large-N_c limit the masses of nucleon and Delta are degenerate. Keeping only the pole terms yields

$$\mathcal{M}_N = -\frac{\sqrt{2}\,g_A^2}{2F_\pi^2}\,\bar{v}_n\gamma^\mu k_\mu u_p\, m_N^2\left(\frac{1}{t-m_N^2}+\frac{1}{u-m_N^2}\right) \tag{A.3}$$

and

$$\begin{aligned}
\mathcal{M}_\Delta = &-\frac{\sqrt{2}\,h_A^2}{4\cdot 9\,F_\pi^2} \\
&\times\left(\bar{v}_n u_p\, 3\,(s-2m_\pi^2)\,m_N\left(\frac{1}{t-m_N^2}-\frac{1}{u-m_N^2}\right)\right. \\
&\left.+\bar{v}_n\gamma^\mu k_\mu u_p\, 2\,m_N^2\left(\frac{1}{t-m_N^2}+\frac{1}{u-m_N^2}\right)\right).
\end{aligned} \tag{A.4}$$

Recalling the large-N_c relation $h_A = 3g_A/\sqrt{2}$ and the fact that the $\bar{v}_n u_p$ term does not contribute to the magnetic amplitude, we observe that indeed $T_M^\Delta = T_M^N/2$.

The calculation of the electric amplitude is slightly more complicated. We will show in the following that for the Delta exchange the $\bar{v}_n u_p$ term contributes (-3) times the other term. In this way the Delta contribution to the electric amplitude is given by $-3+1=-2$ times the $\bar{v}_n\gamma^\mu k_\mu u_p$ structure. This in turn leads to $T_E^\Delta = -T_E^N$ as it should be.

We address the ratio of the two terms in (A.4) for the electric case. We obtain

$$\begin{aligned}
&\frac{\bar{v}_n u_p\, 3\,(s-2m_\pi^2)\,m_N\,(u-t)}{\bar{v}_n\gamma^3 k_3 u_p\, 2\,m_N^2\,(u+t-2m_N^2)} \\
&\approx \frac{m_N\, 3\,(s-2m_\pi^2)\,m_N\,(u-t)}{p_z\,(-2p_{\text{c.m.}}\cos\theta)\,2\,m_N^2\,(u+t-2m_N^2)} \\
&= \frac{3\,(s-2m_\pi^2)}{u+t-2m_N^2} = -3
\end{aligned} \tag{A.5}$$

as claimed.

Appendix B. Cut structure of resonance pole terms

The t- and u-channel pole terms cause left-hand cuts in the $\bar{\Lambda}\Sigma \to 2\pi$ amplitudes. It is worth to figure out in particular the cut structure of the resonance-exchange terms since a meaningful matching of these terms to χPT requires to avoid as much as possible the cuts and the effects/structures caused by them. The starting points of the cuts are given by solutions of the equation

$$\left(-\frac{1}{2}\,s+\frac{1}{2}\,m_\Sigma^2+\frac{1}{2}\,m_\Lambda^2+m_\pi^2-m_{\Sigma^*}^2\right)^2-4\,p_z^2\,p_{\text{c.m.}}^2=0. \tag{B.1}$$

Analytical formulae could be provided for these starting points of the cuts (solutions of a quadratic equation in s), but we will not present them here. Instead we present the numerical values for points that are of relevance for the resonance-exchange contributions to the $\bar{\Lambda}\Sigma \to 2\pi$ amplitudes. The (pseudo-)thresholds are given by

$$s_1 = (m_\Sigma - m_\Lambda)^2 \approx 0.00592\,\text{GeV}^2,$$
$$s_2 = (2m_\pi)^2 \approx 0.0779\,\text{GeV}^2,$$
$$s_3 = (m_\Sigma + m_\Lambda)^2 \approx 5.33\,\text{GeV}^2. \tag{B.2}$$

There are two cuts. One ranges from $-\infty$ to $s_{c1} \approx -0.105\,\text{GeV}^2$, the other from $s_{c2} \approx -0.00305\,\text{GeV}^2$ to zero. The magnetic amplitude has cusps at s_{c1}, s_{c2} and zero. (The electric amplitude diverges at s_{c1} and s_{c2}.) The very small cut from s_{c2} to zero has (only) an impact on the region around $s = 0$. Thus a matching to χPT should be performed for small values of s but for $|s| \gg |s_{c2}|$. One possibility is a matching at the two-pion threshold $s_2 = (2m_\pi)^2$. A second possible choice is a matching for negative s with $s_{c1} \ll s \ll s_{c2}$. For the latter case a reasonable choice might be to use the threshold value for t of the reaction $\Sigma\pi \to \Lambda\pi$. The threshold of this reaction is at $m_\Sigma + m_\pi$ and there the value of the momentum transfer from the pions to the baryons is given by

$$s_{t0} = -m_\pi(m_\Sigma^2 - m_\Lambda^2)/(m_\Sigma + m_\pi) \approx -0.0186\,\text{GeV}^2, \tag{B.3}$$

which lies comfortably between s_{c1} and s_{c2}.

A third possibility is a theoretical calculation with an appropriate low-energy limit. In the limit $m_\pi \to 0$ the small cut between s_{c2} and zero disappears. Only one cut is left that ranges from $-\infty$ to

$$s_c = -\frac{m_{\Sigma^*}^4 - (m_\Sigma^2 + m_\Lambda^2)\,m_{\Sigma^*}^2 + m_\Sigma^2 m_\Lambda^2}{m_{\Sigma^*}^2}. \tag{B.4}$$

Thus in this limit one can perform a matching at $s = 0$. If one puts m_π to zero it makes sense to also neglect the mass difference between m_Σ and m_Λ. Otherwise the two pseudo-thresholds at s_1 and s_2 would change their ordering. After this double limit $m_\pi \to 0$ and $m_\Lambda \to m_\Sigma$ one can evaluate the resonance-pole contribution to the magnetic amplitude for $s = 0$. One obtains

$$
\begin{aligned}
K_{\text{res,low}}^M &:= \lim_{s \to 0} \lim_{m_\Lambda \to m_\Sigma} \lim_{m_\pi \to 0} K_{\text{res}}^M(s) \\
&= \frac{h_A^2}{24\sqrt{3}F_\pi^2}\,\frac{(-m_{\Sigma^*}^2 + 4m_{\Sigma^*}m_\Sigma - m_\Sigma^2)(m_{\Sigma^*} + m_\Sigma)}{m_{\Sigma^*}^2(m_{\Sigma^*} - m_\Sigma)}.
\end{aligned}
\tag{B.5}
$$

Matching is then performed according to (29).

A detailed inspection of the magnetic amplitude (not displayed here) shows that the "distortion" of the curve caused by the small cut is of minor importance at s_{t0} and at s_2. In the vicinity of s_1 there are no cuts, but there is already a large slope. Thus a matching to χPT at s_1 would not be a good choice. Numerically the ratio between the amplitudes at s_2 and at s_{t0} is about 0.78. The ratio between the magnetic amplitude at s_{t0} and (B.5) is

about 0.97, *i.e.* very close to 1, demonstrating agreement between the idea to match at the physically reasonable point s_{t0} and the theoretical low-energy calculation (B.5). For our numerical results we will use the analytical expression (B.5). Note, however, that in view of the large uncertainties in b_{10} a matching at the two-pion threshold would also be a reasonable choice.

References

1. Particle Data Group (C. Patrignani *et al.*), Chin. Phys. C **40**, 100001 (2016).
2. V. Punjabi, C.F. Perdrisat, M.K. Jones, E.J. Brash, C.E. Carlson, Eur. Phys. J. A **51**, 79 (2015) arXiv:1503.01452.
3. R. Pohl *et al.*, Nature **466**, 213 (2010).
4. C.E. Carlson, Prog. Part. Nucl. Phys. **82**, 59 (2015) arXiv:1502.05314.
5. R. Frisch, O. Stern, Z. Phys. **85**, 4 (1933).
6. V. Pascalutsa, M. Vanderhaeghen, S.N. Yang, Phys. Rep. **437**, 125 (2007) arXiv:hep-ph/0609004.
7. M. Gell-Mann, Phys. Lett. **8**, 214 (1964).
8. B. Kubis, U.G. Meißner, Eur. Phys. J. C **18**, 747 (2001) arXiv:hep-ph/0010283.
9. S.J. Brodsky, G.R. Farrar, Phys. Rev. D **11**, 1309 (1975).
10. PANDA Collaboration (M.F.M. Lutz *et al.*), arXiv:0903.3905 (2009).
11. HADES Collaboration (M. Lorenz *et al.*), J. Phys. Conf. Ser. **668**, 012022 (2016).
12. T. Husek, S. Leupold, in preparation (2017).
13. S. Weinberg, Physica A **96**, 327 (1979).
14. J. Gasser, H. Leutwyler, Ann. Phys. **158**, 142 (1984).
15. J. Gasser, H. Leutwyler, Nucl. Phys. B **250**, 465 (1985).
16. S. Scherer, Adv. Nucl. Phys. **27**, 277 (2003) arXiv:hep-ph/0210398.
17. S. Scherer, M.R. Schindler, Lect. Notes Phys. **830**, 1 (2012).
18. V. Pascalutsa, M. Vanderhaeghen, Phys. Lett. B **636**, 31 (2006) arXiv:hep-ph/0511261.
19. T. Ledwig, J. Martin Camalich, L.S. Geng, M.J. Vicente Vacas, Phys. Rev. D **90**, 054502 (2014) arXiv:1405.5456.
20. J.J. Sakurai, *Currents and Mesons* (University of Chicago Press, Chicago, 1969).
21. G. Colangelo, J. Gasser, H. Leutwyler, Nucl. Phys. B **603**, 125 (2001) arXiv:hep-ph/0103088.
22. R. Garcia-Martin, R. Kaminski, J.R. Pelaez, J. Ruiz de Elvira, F.J. Yndurain, Phys. Rev. D **83**, 074004 (2011) arXiv:1102.2183.
23. C. Hanhart, Phys. Lett. B **715**, 170 (2012) arXiv:1203.6839.
24. S.P. Schneider, B. Kubis, F. Niecknig, Phys. Rev. D **86**, 054013 (2012) arXiv:1206.3098.
25. F. Stollenwerk, C. Hanhart, A. Kupsc, U. Meißner, A. Wirzba, Phys. Lett. B **707**, 184 (2012) arXiv:1108.2419.
26. C. Hanhart, A. Kupsc, U.G. Meißner, F. Stollenwerk, A. Wirzba, Eur. Phys. J. C **73**, 2668 (2013) arXiv:1307.5654.

27. F. Niecknig, B. Kubis, S.P. Schneider, Eur. Phys. J. C **72**, 2014 (2012) arXiv:1203.2501.
28. X.W. Kang, B. Kubis, C. Hanhart, U.G. Meißner, Phys. Rev. D **89**, 053015 (2014) arXiv:1312.1193.
29. W.R. Frazer, J.R. Fulco, Phys. Rev. **117**, 1609 (1960).
30. P. Mergell, U.G. Meißner, D. Drechsel, Nucl. Phys. A **596**, 367 (1996) arXiv:hep-ph/9506375.
31. M. Hoferichter, B. Kubis, J. Ruiz de Elvira, H.W. Hammer, U.G. Meißner, Eur. Phys. J. A **52**, 331 (2016) arXiv:1609.06722.
32. R. Omnes, Nuovo Cimento **8**, 316 (1958).
33. S. Mandelstam, Phys. Rev. Lett. **4**, 84 (1960).
34. M. Jacob, G. Wick, Ann. Phys. **7**, 404 (1959).
35. M.E. Peskin, D.V. Schroeder, *An Introduction to Quantum Field Theory* (Perseus, Cambridge, Massachusetts, 1995).
36. M. Hoferichter, J. Ruiz de Elvira, B. Kubis, U.G. Meißner, Phys. Rep. **625**, 1 (2016) arXiv:1510.06039.
37. M.F.M. Lutz, E.E. Kolomeitsev, Nucl. Phys. A **700**, 193 (2002) arXiv:nucl-th/0105042.
38. M. Hoferichter, C. Ditsche, B. Kubis, U.G. Meißner, JHEP **06**, 063 (2012) arXiv:1204.6251.
39. U.G. Meißner, S. Steininger, Nucl. Phys. B **499**, 349 (1997) arXiv:hep-ph/9701260.
40. B. Kubis, PhD Thesis, Forschungszentrum Jülich (2003).
41. E.E. Jenkins, A.V. Manohar, Phys. Lett. B **259**, 353 (1991).
42. V. Pascalutsa, R. Timmermans, Phys. Rev. C **60**, 042201 (1999) arXiv:nucl-th/9905065.
43. R.F. Dashen, A.V. Manohar, Phys. Lett. B **315**, 425 (1993) arXiv: hep-ph/9307241.
44. J.A. Oller, M. Verbeni, J. Prades, JHEP **09**, 079 (2006) arXiv: hep-ph/0608204.
45. M. Frink, U.G. Meißner, Eur. Phys. J. A **29**, 255 (2006) arXiv:hep-ph/0609256.
46. S. Weinberg, Phys. Rev. Lett. **17**, 616 (1966).
47. Y. Tomozawa, Nuovo Cimento A **46**, 707 (1966).
48. U.G. Meißner, arXiv:hep-ph/9711365 (1997).
49. N. Wies, J. Gegelia, S. Scherer, Phys. Rev. D **73**, 094012 (2006) arXiv:hep-ph/0602073.
50. S.J. Puglia, M.J. Ramsey-Musolf, S.L. Zhu, Phys. Rev. D **63**, 034014 (2001) arXiv:hep-ph/0008140.
51. A2 Collaboration (P. Adlarson *et al.*), Phys. Rev. C **95**, 025202 (2017).
52. M. Hoferichter, B. Kubis, S. Leupold, F. Niecknig, S.P. Schneider, Eur. Phys. J. C **74**, 3180 (2014) arXiv: 1410.4691.
53. J.M. Alarcón, A.N. Hiller Blin, C. Weiss, arXiv:1701.05871 (2017).
54. J.M. Alarcón, A.N. Hiller Blin, M.J. Vicente Vacas, C. Weiss, arXiv:1703.04534 (2017).
55. C. Granados, C. Weiss, JHEP **01**, 092 (2014) arXiv: 1308.1634.